OPTIMIZATION OF LCF MATERIAL PARAMETERS OF 20MnMoNi55 LOW ALLOY RPV STEEL USING GA IN TANDEM WITH FE SOFTWARE ABAQUS

THESIS SUBMITTED FOR THE FULFILLMENT OF THE DEGREE OF

MASTER OF ENGINEERING

BY

SUBHAYAN MAL

EXAMINATION ROLL NO: M4MEC19014

DEPARTMENT OF MECHANICAL ENGNEERING

FACULTY OF ENGINEERING AND TECHNOLOGY

JADAVPUR UNIVERSITY

KOLKATA, INDIA

MAY, 2019

OPTIMIZATION OF LCF MATERIAL PARAMETERS OF 20MnMoNi55 LOW ALLOY RPV STEEL USING GA IN TANDEM WITH FE SOFTWARE ABAQUS

THESIS SUBMITTED FOR THE FULFILLMENT OF THE DEGREE OF
MASTER OF ENGINEERING
BY

SUBHAYAN MAL

EXAMINATION ROLL NO: M4MEC19014

REGISTRATION NO: 140871 of 2017-18

DEPARTMENT OF MECHANICAL ENGNEERING
FACULTY OF ENGINEERING AND TECHNOLOGY
JADAVPUR UNIVERSITY
KOLKATA, INDIA

MAY, 2019

Blank Page

JADAVPUR UNIVERSITY
KOLKATA – 700032

1. **Title of the Thesis:** OPTIMIZATION OF LCF MATERIAL PARAMETERS OF 20MnMoNi55 LOW ALLOY RPV STEEL USING GA IN TANDEM WITH FE SOFTWARE ABAQUS

2. **Name, Designation and Institution of Supervisor(s):**

Prof. Sanjib Kumar Acharyya
Professor,
Department of Mechanical Engineering,
Jadavpur University.

Blank Page

FACULTY OF ENGINEERING AND TECHNOLOGY

JADAVPUR UNIVERSITY

CERTIFICATE OF RECOMMENDATION

We hereby recommend that the thesis presented under our supervision by **Mr. Subhayan Mal** entitled "**Optimization of LCF Material Parameters of 20MnMoNi55 Low Alloy RPV Steel Using GA in Tandem with FE Software ABAQUS**" be accepted in partial fulfillment of the requirements for the degree of Master of Mechanical Engineering.

……

Prof. Sanjib Kumar Acharyya
Thesis advisor
Dept. of Mechanical Engineering
Jadavpur University

……..
(Dr. Gautam Majumdar)
Professor and Head
Department of Mechanical Engg.
Jadavpur University, Kolkata

……
(Prof. Chiranjib Bhattacharjee)
Dean of faculty council of
Engineering and Technology
Jadavpur University, Kolkata

Blank Page

DEPARTMENT OF MECHANICAL ENGNEERING
FACULTY OF ENGINEERING AND TECHNOLOGY
JADAVPUR UNIVERSITY

CERTIFICATE OF APPROVAL*

The foregoing thesis entitled "**Optimization of LCF Material Parameters of 20MnMoNi55 Low Alloy RPV Steel Using GA in Tandem with FE Software ABAQUS**" is hereby approved as a creditable study of an engineering subject carried out and presented in a satisfactory manner to warrant its acceptance as a prerequisite for the degree of "**Master of Engineering"** at the Department of Mechanical Engineering, Jadavpur University, Kolkata700032, for which it has been submitted. It is understood that by this approval the undersigned do not necessarily endorse or approve any statement made, opinion expressed or conclusion drawn there in but approve the thesis only for the purpose for which it is submitted.

Committee on Final Examination
For Evaluation of the Thesis

Signature of Examiners

*Only in case the recommendation is concurred in

Blank Page

DEPARTMENT OF MECHANICAL ENGNEERING
FACULTY OF ENGINEERING AND TECHNOLOGY
JADAVPUR UNIVERSITY

DECLARATION OF ORIGINALITY AND COMPLIANCE OF ACADEMIC ETHICS

It is hereby declared that the thesis entitled "**Optimization of LCF Material Parameters of 20MnMoNi55 Low Alloy RPV Steel Using GA in Tandem with FE Software ABAQUS**" contains literature survey and original research work by the undersigned candidate, as part of his degree of "**Master of Engineering"** at the Department of Mechanical Engineering, Jadavpur University, Kolkata700032.

All information in this document has been obtained and presented in accordance with academic rules and ethical conduct.

It is also declared that all materials and results, not original to this work have been fully cited and referred throughout this thesis, according to rules of ethical conduct.

Name: **SUBHAYAN MAL**
Registration Number: **140871 of 2017-18**
Examination Roll Number: **M4MEC19014**
Dated: 31.05.2018

(Signature)
SUBHAYAN MAL
Master of Engineering
Department of Mechanical Engineering
Jadavpur University, Kolkata700032

Blank Page

Dedicated to:

My Parents and Teachers

Blank Page

ACKNOWLEDGEMENT

This project is by far the most significant accomplishment in my life and it would be impossible without people who supported me and believed in me.

Foremost, I would like to express my sincere gratitude to my guide ***Dr.Sanjib Kumar Acharyya*** *for the continuous support of my master degree study and Project, for his patience, motivation, enthusiasm, and immense knowledge. His guidance helped me in all the time of project and writing of this thesis. I could not have imagined having a better advisor and mentor for my master degree study.*

*I am very much thankful to my seniors and laboratory-in-charge of the '****Fatigue, Fracture and Damage Analysis Laboratory****' helped me a lot to understand and analysis the enormous testing data and also gave me substantial support in the software part.*

I also thank all of my friends who have more or less contributed to the preparation of this project .I will be always indebted to them.

I would like to thank my parents, who taught me the value of hard work by their own example and give me the opportunity for education.

_____

Subhayan Mal

Blank Page

CONTENTS

CONTENTS

NOMENCLATURE

List of Subscripts and Superscripts

Subscripts		Superscripts	
0	Initial (σ_0 = Initial yield stress)	i	Current or, i^{th}
c	Current (σ_c =Current yield stress) Critical (ρ_c = Critical dislocation density)	e	Elastic
1	Softening	p	Plastic
2	Hardening		
ij	Second order tensor indices		
eq	equivalent		
mises	Von-Mises norm		

List of Prefixes, Operators and Indices

Δ	Increment Range
∂	Partial differential operator
d	Total differential operator
‘	Space derivative
˙	Time derivative or rate
δ	Kronecker delta $\left(\delta_{ij}\right)$

List of Symbols

a	Power law coefficient
m	Power law exponent Mean stress
μ or G	Lame’s parameter or Shear modulus
E	Young’s modulus
λ	Lame’s parameter Non-negative plastic multiplier (dλ) Softening Coefficient (Marquis approach) Slip band width
ν	Poisson’s ratio

σ Stress

ε Strain

S Deviatoric stress

α Deviatoric back stress (α_{ij})

ϕ Yield function

R Isotropic hardening stress

h Modulus of plasticity

n Flow vector $\left(n_{ij}\right)$

n* Normal direction to the plastic strain memory surface

LIST OF TABLES

LIST OF FIGURES

LIST OF FIGURES

Blank Page

Chapter 1. Introduction

1.1 Introduction

Most engineering components fail due to fatigue (G.Dieter, 1961). The fatigue damage shows no visible warning before failure.Fatigue is quite structure sensitive, it not only depends on the specimen shape and size (Shuhei NOGAMI, Yuki SATO, 2010) but on the microstructure(Hideaki Shibata, Hirohisa Shiota, 1996) also. Rigorous testing for fatigue life is not always possible for every possible specimen geometry, and there comes the necessity of Finite Element (FE) simulation. In FE simulations, the specimen geometry need no restriction and the process is quite cost effective and time saving with comprehended strategic modelling.

Prediction of fatigue life for a component in FE simulation requires accurate calculation of deformation and carefully constructed constitutive relations. Standard FE software calculate the deformation with a reliable accuracy (ABAQUS Manual, v6.8). On the other hand, the user can choose or design the constitutive relations for a material behaviour,and there inevitably comes the in-depth understanding of the microstructural behaviour of the material. In present days, modeling of the material behavior is becoming increasingly important in predicting possible failure conditions in engineering components and consequently, optimization of their design.

The material, 20MnMoNi55 low alloy steel, is a designed RPV material with high fracture toughness, strength and ductility (M. S. E1-Fadaly, T.A. E1-Sarrage, A.M. Eleiche, W. Dahl, 1995). The typical application (nuclear reactor pressure vessel) of the material may involve cyclic loading during start up or shut down sequence or due to seismic activity. The material may experience plastic loading at microstructural level (near a stress concentration point like micro-crack, inclusion, grain boundary etc.) even for a low loading amplitude. Therefore, study of the low cycle fatigue behaviour of the material is a safety-critical issue.

1.2 Fundamentals of Cyclic Plasticity

Early in the 19th century the concept of fatigue draws the attention of researchers working mainly on mining and railway industries. The first known contribution is made by a German
engineer, named W. A. J. Albert in 1837 (Pook, 2007) devised a testing machine for hoist chains used in mines and published the first article on fatigue. The first fatigue test results published in English appear to be those by Fairbairn (1864) on repeated bending fatigue tests on beams. Rankine (1842) recognized the importance of stress concentrations during investigation of the Versailles Train Crash incident. Braithwaite (1854) reported common service fatigue failures and coined the term ‘fatigue’. Ewing (1903) demonstrated the origin

of fatigue failure in microscopic cracks. Basquin (1910) proposed a log-log relationship for S-N curves, using Wöhler's (1870) test data. Miner (1945) popularized Palmgren's (1924) linear damage hypothesis as a practical design tool for fatigue. If applied load amplitude is low enough to deform the material only elastically, the material survives a large number of cycles, and known as 'High Cycle Fatigue' (HCF).Fatigue is the localized and progressive structural damage. The fatigue damage is cumulative and the materials do not recover when relieved (Palmgren, 1924; Miner, 1945). Eventually a crack will grow unto a critical size and then propagates suddenly to catastrophic fractures.

For quasi-static loading (with low strain-rate at room temperature and in the standard environment), if the applied cyclic load is high enough to deform the material irreversibly (plastically), it survives relatively low number of cycles, and known as 'Low Cycle Fatigue' (LCF). LCF as a material failure process has received much attention since the early work of Manson (1953) and Coffin (1954) where they explained fatigue crack-growth in terms of plastic strain in the tip of cracks.

1.2.1 Experimental Observations for symmetric uniaxial loading

It is observed and experienced that fatigue damage involving plasticity (LCF) grows faster and shows different stress-strain behaviour during the fatigue life (G. Dieter, 1961) before catastrophic failure. These material responses are of practical interest in design of power plant and other engineering components, as sometimes, they indicate the symptoms of any secondary damage mechanism evolved and influencing the fatigue life.

1.2.1.1 Bauschinger effect

The common experimental observations of cyclic plasticity for metals that stress-strain behaviour shows a closed hysteresis loop with reduction in strength after load reversal, called Bauschinger effect (Bauschinger, 1881 and 1886).

If the yield limit is marked asσ_y, then the material during unloading from maximal axial stress state σ_1 behaves elastically up to the point, where the difference between maximal and immediate stress $\sigma_1 - \sigma_2$ is equal to the double of yield limit $2\sigma_y$

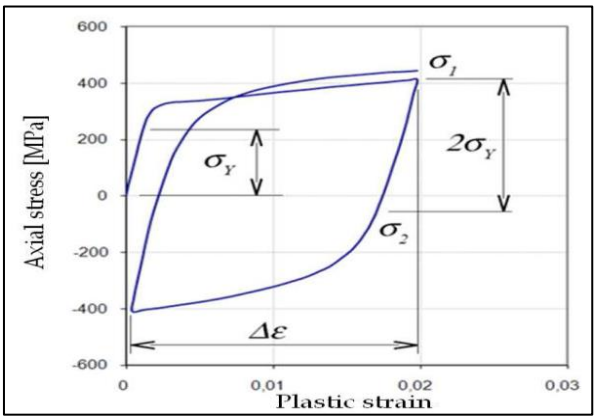

Fig.1.1: *Presentation of Bauschinger effect.*

Kinematic hardening (KH) rules are designed to model closed stress-strain hysteresis loops with Bauschinger effect.

1.2.1.2 Cyclic hardening/softening

Results of the micro structural changes in the beginning stage of cyclic loading are changes of physical properties and stress response in the material. Cyclic softening/hardening effect relates to softening/hardening of material response or decreasing/increasing of resistance against material deformation under cyclic loading. Its intensity usually decrease with number of cycles until the saturated state is reached. During uniaxial cyclic loading, the condition is characterized by closed hysteresis loop. Transient responses in initial cycles caused by cyclic hardening/softening under plastic strain control and stress control are shown at the fig.2

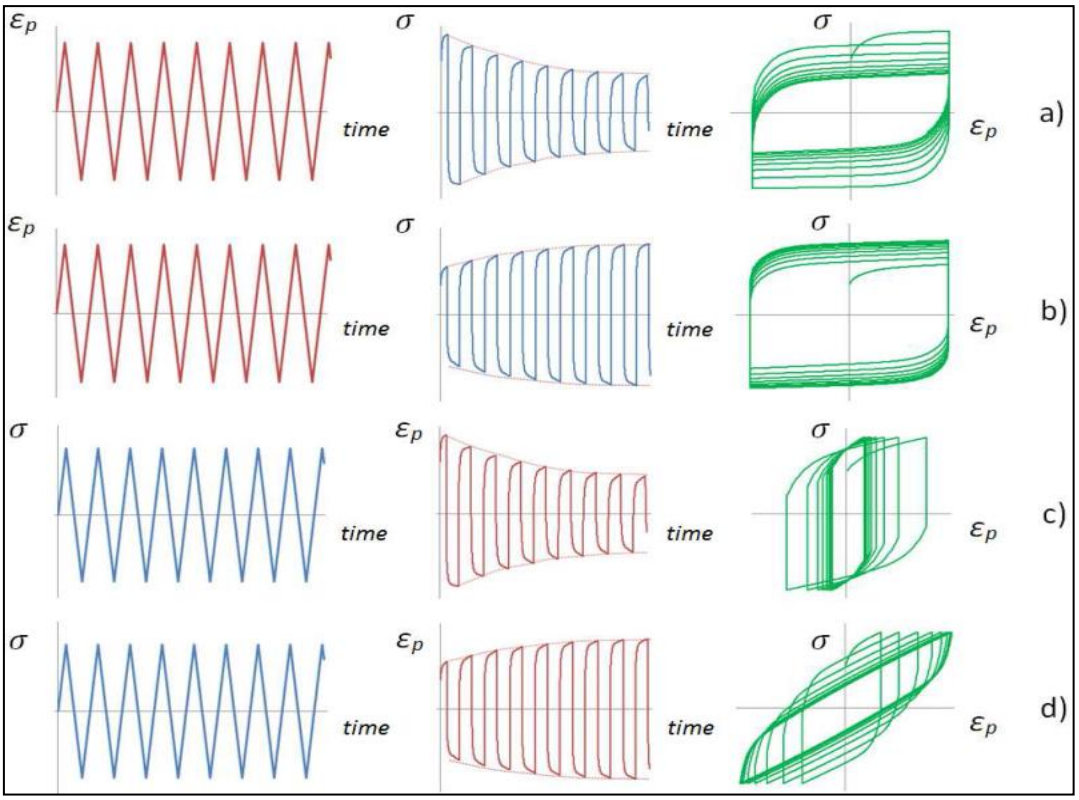

Fig.1.2: *Uniaxial fatigue test material response: a) cyclic softening and b) cyclic hardening under plastic strain controlled loading and c) cyclic hardening and d) cyclic softening under stress controlled loading.*

Some materials show very strong cyclic softening/hardening (stainless steels, cooper, etc.)some less obvious (structural steels). There can be also notable cyclic hardening in certain cycles range and in the remaining lifetime cyclical softening. Properties of cyclic hardening/softening don‘t depend only on material microstructure, but also on loading amplitude or more generally on previous strain history. Such transient behavior of material makes accurate stress-strain modeling more difficult. There is very often mentioned possibility of transient stress-strain behavior estimation according to its strength limit and yield limit ratio, but also very simple hypothesis is used, claiming that hard material cyclically softens whereas soft material cyclically hardens.

1.2.1.3Masing behavior

A material obeys Masing behavior (Masing, 1923; Elline and Kujawaski, 1984; Wang and Laird, 1988) when the upper branches of hysteresis loops with different strain ranges after alignment in lower peaks overlap. More accurately, in the ideal case, single solid curve is created. From microscopic point of view Masing behavior indicates stable microstructure in fatigue process. Most steel materials haven't Masing behaviour. Some engineering materials show Masing behaviour under certain testing conditions. As can be seen from the Fig.3, where the upper branches of hysteresis loops of the investigated material displays non-Masing behaviour depending on the amplitude of plastic strain.

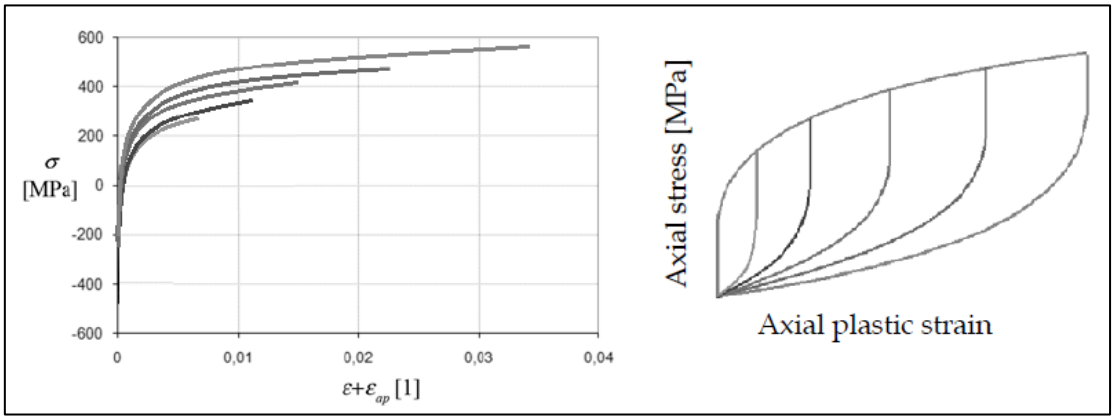

Fig.1.3:*Schematic representation of non-Masing behaviour and Masing behaviour.*

For different complexity in loading condition and for different geometry the material may show many different stress-strain behaviour.

1.2.2 Constitutive modeling for symmetric uniaxial loading

Different cyclic behaviours are observed and documented in the last a few decades of rigorous research for different materials. At the same time, an even more meticulous effort was given to model the phenomena mostly from phenomenological and thermodynamic point of view.

Cyclic plasticity is considered as one of the most critical structural problems to be simulated. And in the context of constitutive modelling, the development of kinematic hardening rule is enormous benchmark in the history of cyclic plasticity modelling. But, some of the cyclic plasticity behaviour of materials are best modelled by isotropic hardening mechanisms, like cyclic hardening/softening, non-proportional hardening etc.

1.2.2.1 Basics of incremental theory of plasticity

For a homogeneous, isotropic and linearly elastic material, the plasticity analysis of the material is introduced by a suitable yield criterion $\sigma_{eq} = \sigma_0$. Here, σ_{eq} is the equivalent stress and $\sigma_0$is the initial yield stress. Mathematically, $\sigma_{eq} - \sigma_0 = 0$ repeats the same condition with a function on the left hand side, known as the yield function ϕ.

Beyond the elastic limit, where small displacement and small strain (less than 5% strain) analysis is applicable, the incremental total strain can be additively decomposed (even when large rigid body rotations are involved with small strains, this simple algebraic decomposition of strains does not yield accurate results) into elastic and plastic strain components$\left(d\varepsilon_{ij}^{tot} = d\varepsilon_{ij}^{e} + d\varepsilon_{ij}^{p}\right)$. Therefore, a general approach to find out actual state of stress at any instance is by applying generalized Hooke's law on the elastic part of the strain and mathematically,

$$\sigma_{ij} = \sigma_{ij}^{0} + 2\mu\left(d\varepsilon_{ij}^{tot} - d\varepsilon_{ij}^{p}\right) + \lambda\, d\varepsilon_{kk}^{tot} \qquad (1.1)$$

Where, σ_{ij}^{0} is the state of stress obtained at last converged time step and, μ and λ are tow material parameters (called Lame's parameters). As for metallic material, it is observed that, the incompressible plasticity assumption holds good $\Big($plastic deformation is purely deviatoric, $\left(\varepsilon_{ij}^{p}\delta_{ij} = 0\right)\Big)$ and therefore, von-Mises yield criterion is widely applicable. As a result, $d\varepsilon_{kk}^{tot}$ is purely elastic$\sum(\, d\varepsilon_{11}^{e} + \, d\varepsilon_{22}^{e} + \, d\varepsilon_{33}^{e})$.

Incompressibility hypothesis endorse no effects of the hydrostatic stress component on yielding and the plastic deformation. Hence, the distortion energy criterion is considered suitable in this case. In its simplest form, in case of perfectly plastic (no hardening) incompressible material, the von-Mises yield function is read as: $\phi = \sigma_{eq} - \sigma_0 = \left[\frac{3}{2}S_{ij}S_{ij}\right]^{1/2} - \sigma_0$, where, S_{ij} are the deviatoric stress components or reduced state of stress. The yield function is represented by an open cylinder of radius σ_0, on π-plane in the deviatoric stress space.

For the work hardening material (metals), the complete quantification of the plastic strain is dependent on the hardening characteristics of the material. Hill (1950) assumed that the resistance to the distortion is measured by the isotropic expansion of yield surface during plastic flow retaining its shape and position with respect to the hydrostatic state of stress. On the other hand, Prager (1955, 1956) proposed a different hardening rule which considers the yield surface can move in the stress space in any direction of strain increment retaining its shape and size. Considering both the hardening mechanisms, the von-Mises yield function becomes:

$$\phi \;= \left[\frac{3}{2}\left(S_{ij} - \alpha_{ij}\right)\left(S_{ij} - \alpha_{ij}\right)\right]^{1/2} - \sigma_c \;=\; 0 \qquad (1.2)$$

here, α_{ij} are deviatoric back stress components respectively. Current yield stress σ_c is additively decomposed into initial yield stress (σ_0) and isotropic hardening/softening (R).

The hardening rules specifically describe the evolutions of isotropic hardening stress and/or back stress (kinematic hardening) components.

For work-hardening materials, Hill (1950) developed the complete stress-strain equation in a more general manner as:

$$d\varepsilon_{ij} = \left[\frac{dS_{ij}}{2G} + \frac{(1-2\nu)}{E}\delta_{ij}\, d\sigma_m\right] + \left[\frac{3}{2}S_{ij}\frac{d\varepsilon_{eq}^{p}}{\sigma_{eq}}\right].$$

Contemporarily, for plastic deformation of the perfectly plastic (neutrally stable) or strain hardening (stable) material, Drucker (1950, 1951, 1959) proposed a stability postulate, which is represented as:$d\sigma_{ij}d\varepsilon_{ij}^{p} \geq 0$. The postulate practically restricts the possibility of material softening and hence instability. Drucker's postulate is broader than the statement summarizes. It confirms the convexity of yield surface and suggests the maximum plastic dissipation (von-Mises, 1928; Taylor, 1947; and Hill, 1948). Consequences of the maximum plastic dissipation postulate are of the highest importance in the plasticity theory. The normality of the plastic flow direction to the potential surface can be directed from the principle of maximum plastic dissipation.

The possibility and direction of plastic strain increment (plastic flow) for strain-hardening material is generally directed by the flow rule. The possibility and quantification of the plastic flow is ascertained by a non-negative scalar ($d\lambda$) similarly as in Prandtl-Reuss equation. It can be shown that the plastic multiplier is actually the equivalent plastic strain increment. Though, the complete quantification of the plastic strain magnitudes are dependent on the specific hardening rules and consistency condition. From the normality rule, the direction of the plastic flow, called the flow vector (n_{ij})in plasticity analysis, is determined by the gradient of the potential surface in the stress direction. For von-Mises plasticity for metals, the flow rule is called the associative or associated flow rule when the yield surface is identical to the potential surface. The equation of the associated plastic flow is finally written as:

$$d\varepsilon_{ij}^{p} = d\lambda\frac{\partial\phi}{\partial S_{ij}} \tag{1.3}$$

The consistency condition implies that the plastic deformation occurs for the state of stress is to be in such a way that their equivalent always lies on the revised yield surface. The hypothesis enables the quantification of the plastic multiplier ($d\lambda$) for associated flow.

The condition is mathematically presented as: $\phi + d\phi = 0$, in yielded condition, $\phi = 0$, therefore, $d\phi = 0$ and expressed as:

$$d\phi = \frac{\partial\phi}{\partial S_{ij}}dS_{ij} + \frac{\partial\phi}{\partial\alpha_{ij}}d\alpha_{ij} + \frac{\partial\phi}{\partial\sigma_c}d\sigma_c = 0 \tag{1.4}$$

The plastic modulus is of great importance when the equivalent plastic strain increment $\left(d\varepsilon_{eq}^{p}\right)$ is computed using Newton iterative method in numerical simulations.

The plastic modulus is formulated from the consistency condition ($d\phi = 0$)conforming associative flow rule$\left(d\varepsilon_{ij}^{p} = d\lambda \frac{\partial \phi}{\partial S_{ij}}\right)$and incorporating the specific hardening laws as:

$$h = n_{ij} \frac{dS_{ij}}{d\varepsilon_{eq}^{p}} = n_{ij} \frac{d\alpha_{ij}}{d\varepsilon_{eq}^{p}} + \frac{d\sigma_c}{d\varepsilon_{eq}^{p}} \tag{1.5}$$

where, $n_{ij} = \frac{\partial \phi}{\partial S_{ij}} = \frac{3}{2}\frac{S_{ij}}{\sigma_{eq}}$ and, $d\varepsilon_{eq}^{p} = \left[\frac{2}{3} d\varepsilon_{ij}^{p} d\varepsilon_{ij}^{p}\right]^{1/2}$. In case of cyclic plasticity kinematic hardening rules are required to simulate stress-strain hysteresis loop along with the Bauschinger effect. The non-Masingbehaviour can also be addressed by varying the kinematic hardening parameters. Though sometimes, when the material is only non-Masing at the elastic limit, the behaviour can be captured introducing isotropic hardening rule. Though the primary objective of incorporating isotropic hardening is to simulate cyclic hardening/softening behaviour. In case of saturated loops, it is observed that, the cyclic hardening/softening gets saturated, there kinematic hardening alone can simulate the stress-strain hysteresis loop accurately. In the subsequent analysis later, the specific kinematic hardening law suitable for the material and its parametric quantification are discussed.

1.2.2.2 Kinematic hardening model

Translation of the yield surface in the deviatoric stress space known as the kinematic hardening mechanism. The most of the cyclic plasticity phenomena are modelled by modifying the kinematic hardening rule. In the following sections, a brief history of such modifications are presented.

The standard kinematic hardening rules include the forest pile-ups of dislocations as 'back stress' and the effect of annihilated mobile dislocations causing some recovery of the back stress is generally included in the ‘dynamic recovery’ term. The concept of KH rule is materialized first in the work of Prager (1956).

1.2.2.2.1Linear kinematic hardening rule - Prager’s model

Prager (1955) proposed the linear kinematic hardening model which assumes collinear relation between increments of the back stress (kinematic variable) components$(d\alpha_{ij})$ and the increments of the plastic strain components$\left(d\varepsilon_{ij}^{p}\right)$.

$$d\alpha_{ij} = \frac{2}{3} C \, d\varepsilon_{ij}^{p} \tag{1.6}$$

The initial hardening modulus,C, is temperature dependent material parameter. The yield surface, under applied load which causes the plastic deformation, translates to a new location. The initial center is translated by equivalent back stressα.

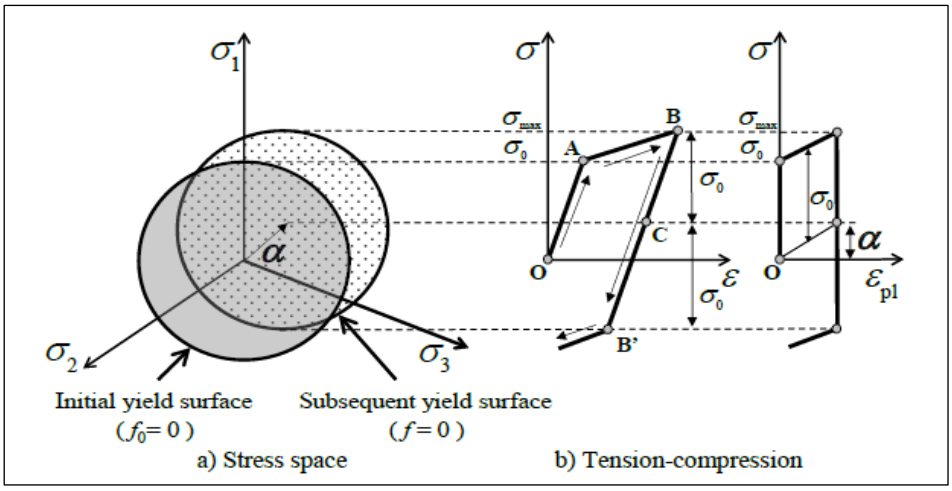

Fig.1.4: *Evolution of the linear kinematic hardening model*

The Prager's model is schematically illustrated in Fig.1.A specimen which is firstly loaded up to the point *B* and then unloaded and loaded in the reverse direction until the point *B'*. Both the elastic and the plastic deformations occur in the point *B* while only the elastic deformation appears between the points *B* and *B'*. However, the elasto-plastic deformation occurs again when an applied load passes the point *B'*further. Radius of the yield surface is equal to the initial yield stress confirming that the linear kinematic hardening model is able to capture the Bauschinger effect.

The main advantage of this model is having only one material parameter, C.The linear KH rule by Prager (1956) simulates the Bauschinger effect with a closed hysteresis loop but it fails to simulate the non-linearity of the material response in the post-elastic regime.

For improved simulation of the non-linear stress-strain curve many attempts were made. Overlay modelby Besseling(1958) is most considerable amongst them. The model proposes a multilinear construction but lacks the physical significance. Instead, the model with a single yield surface with a non-linear evolution equation of internal variables provides physical significance and results in more robust outcome in simulation. The non-linear kinematic hardening rules became widely popular.

1.2.2.2.2 Non-linear Armstrong-Frederick (AF)model

Armstrong and Frederick (1966) proposed that back stress components are the results of two different micro-mechanisms namely hardening and dynamic recovery of internal state variables which is dependent on the effective plastic deformation and the state of back stress. The increment of the back stress components are:

$$d\alpha_{ij} = \frac{2}{3} C\, d\varepsilon_{ij}^{p} - \gamma\, \alpha_{ij} d\varepsilon_{eq}^{p} \qquad (1.7)$$

Where C and γare material parameters. The quantity dp is an increment of equivalent plastic strain, expressed as:$d\varepsilon_{eq}^{p} = \sqrt{\frac{2}{3}\, d\varepsilon_{ij}^{p}\, d\varepsilon_{ij}^{p}}$.

A proportional stress raiser by dislocation pile-ups may be apprehended by the first term on the right hand sides of Eq.1.7, as observed identical to the Prager model. When a material is loaded beyond its yield limit, microscopically, a large number of dislocations are activated by generation and multiplication at different sources, like, grain and sub-grain boundaries, pinned dislocations, impurities, and other kind of defects etc. As plastic deformation continues, the probability of mobile dislocations being tangled with each other and caught up in the dislocation forest increases exponentially as more slip systems get activated. The entanglement of mobile dislocations at different sites resist the easy glide of dislocations, cumulatively resulting the macroscopic hardening.

Transmission Electron Microscope (TEM) micrographs can show, other than entanglement, when dislocations of opposite signs interact, they both get annihilated (Essmann and Mughrabi, 1979) reliving the stored energy and space for remaining dislocations to glide easily without barrier. Movable dislocations within a slip system (slip direction and plane) when interact with each other and dislocations of opposite signs annihilate, the process is designated as 'dynamic recovery'. The second term on the right hand side of the Eq.1.7 gives the dynamic recovery contribution for Armstrong-Frederick KH model. Any kinematic hardening (KH) rule used in the material modelling, now a days, are equipped with the hardening term that handles the dislocation generation and pile ups and a recovery term mainly capture the annihilation of movable dislocations within the active slip systems.

For the uniaxial loading case, the von Mises yield condition becomes to the simpler form. Similarly we can modify nonlinear kinematic hardening rule if we will consider only deviatoric part of the equation (1.7) taking into account plastic incompressibility. Then the nonlinear kinematic hardening rule leads to the differential equation $d\alpha = Cd\varepsilon_p - \gamma\alpha\left|d\varepsilon_p\right|$. To dispose of the absolute value of α, a multiplier $\psi = \pm 1$ can be used and the Eq.1.7 becomes:

$$d\alpha = C\, d\varepsilon_p - \gamma\, \alpha\, \left|d\epsilon_p\right| = C\, d\varepsilon_p - \psi\, \gamma\, \alpha\, d\varepsilon_p$$

Separating the variables, $\int_{\alpha_0}^{\alpha} \frac{d\alpha}{C-\psi\gamma\alpha} = \int_{\varepsilon_0}^{\varepsilon} d\varepsilon_p$ and integrating, we get:

$$\alpha = \frac{C}{\gamma} + \left(\alpha_0 - \psi\frac{C}{\gamma}\right) e^{-\psi\gamma(\varepsilon_p - \varepsilon_{p0})} \tag{1.8}$$

Therefore, the relation for stress is given by yield condition $\sigma = \alpha + \psi\sigma_y$. For tension $\psi = +1$ and considering zero initial values of plastic strain $\left(d\varepsilon_p^0 = 0\right)$ and back stress $(d\alpha^0 = 0)$, the Eq.1.8 becomes $\sigma = \sigma_y + \frac{C}{\gamma}(1 - e^{-\gamma\varepsilon_p})$. Now, we can investigate the limit values of the nonlinear function and its first derivation to get a concept about influence of parameters C and γ on stress – strain response of the Armstrong-Frederick model:

$$\lim_{\varepsilon_p \to 0} Ce^{-\gamma\varepsilon_p} = C \text{ and, } \lim_{\varepsilon_p \to \infty} \sigma_y + \frac{C}{\gamma}(1 - e^{-\gamma\varepsilon_p}) = \sigma_y + \frac{C}{\gamma}$$

Described nonlinear kinematic hardening model allows to correctly capture Bauschinger effect and even behavior by nonsymmetrical loading in tension-compression. The big advantage of Armstrong-Frederick model is its easy implementation despite the nonlinear behavior.

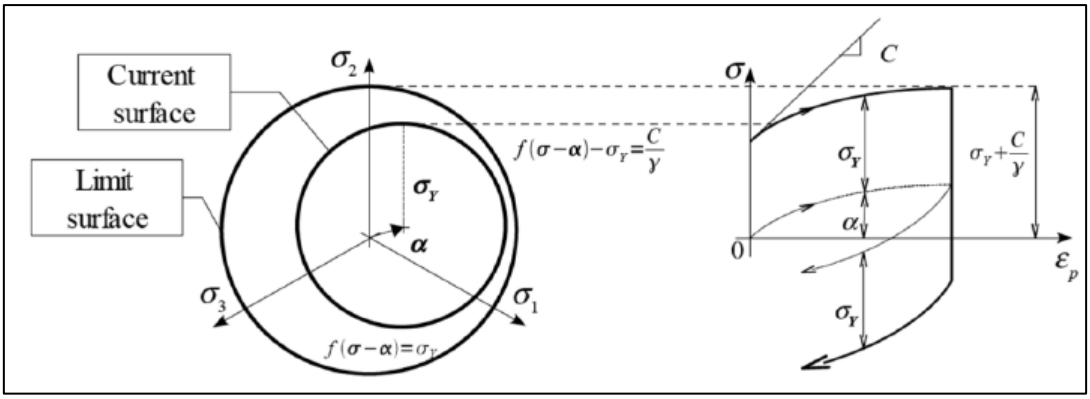

Fig.1.5: *Properties of the nonlinear kinematic hardening model of Armstrong-Frederick.*

On the other hand, the model cannot describe the hysteresis loop shape precisely. For the case of cyclic loading the parameters σ_y, C and γ should be estimated from the cyclic strain curve. It is possible to determine the equation corresponding to the cyclic curve of Armstrong-Frederick model by application of equation (1.8) for the upper branch and the bottom branch of hysteresis loop. For tension $\psi = 1$ is valid and we have:

$$\alpha_{max} = \frac{C}{\gamma} + \left(\alpha_{min} - \frac{C}{\gamma}\right) e^{-\gamma(\varepsilon_p - \varepsilon_{ap})} \tag{1.9}$$

For the compression ($\psi = -1$) similarly,

$$\alpha_{min} = -\frac{C}{\gamma} + \left(\alpha_{max} + \frac{C}{\gamma}\right) e^{\gamma(\varepsilon_p - \varepsilon_{ap})} \tag{1.10}$$

Substituting Eq.1.9 into Eq.1.10, $\sigma_a = \sigma_y + \frac{C}{\gamma} tanh(\gamma \varepsilon_{ap})$, where, $tanh(x)$ is the hyperbolic tangent function and $\sigma_a, \varepsilon_{ap}$ are stress amplitude and plastic strain amplitude respectively.

Single surface non-linear Armstrong-Frederick KH model shows rudimentary simulations of the stress-strain hysteresis curvature and over-predictions in the uniaxial ratcheting response.

1.2.2.2.3Chaboche model – Segmented Armstrong-Frederick rule

Chaboche and his co-workers (1979, 1989, 1991, and 1994) proposed a 'decomposed' nonlinear kinematic hardening rule. Chaboche kinematic hardening rule is a superposition of several Armstrong-Frederick hardening rules.

The total back stress, through superposition of m segments, is:

$$d\alpha_{ij} = \sum_{k=1}^{m} d\alpha_{ij}^{k} \tag{1.11}$$

Where, each segment evolves according to the Armstrong and Frederick rule for material parameters C^k and γ^k for k^{th}segment:

$$d\alpha_{ij}^{k} = \frac{2}{3}\, C^k\, d\varepsilon_{ij}^{p} - \gamma^k\, \alpha_{ij}^{k}\, d\varepsilon_{eq}^{p} \tag{1.12}$$

A stable hysteresis curve can be divided into three critical segments. The initial high modulus at the onset of yielding, the constant modulus segment at a higher strain range and the transient nonlinear segment. Accordingly, the first rule $\left(d\alpha_{ij}^{1}\right)$ should start hardening with a very large modulus and stabilizes very quickly. The second rule $\left(d\alpha_{ij}^{2}\right)$ should simulate the transient nonlinear portion of the stable hysteresis curve. Finally, the third rule $\left(d\alpha_{ij}^{3}\right)$should be a linear hardening rule $(\gamma^3 = 0)$to represent the subsequent linear part of the hysteresis curve at a high strain range. If this scheme is followed, the simulation for a stable hysteresis loop improves. Chaboche model has a tendency to over-predict uniaxial ratcheting rates during initial cycles and over-predicts the biaxial cases to a large extent. Chaboche (1991) added a fourth hardening rule with a concept of 'threshold' in his model. This kinematic hardening rule grows linearly to a certain 'threshold' stress level and subsequently hardens according to the Armstrong-Frederick rule. It is observed that the incorporation of a fourth rule improves the stable hysteresis loop simulation, but the ratcheting simulations for both uniaxial and biaxial experiments do not improve that much.

Due to the usage of Armstrong-Frederick evolution law we can directly write the expression for static strain curve

$$\sigma = \psi\sigma_y + \sum_{i=1}^{M} \psi\frac{C_i}{\gamma_i} + \left(\alpha_0^{(i)} - \psi\frac{C_i}{\gamma_i}\right) e^{-\psi\gamma_i(\varepsilon_p - \varepsilon_{p0})} \tag{1.13}$$

and for cyclic strain curve$\sigma_a = \sigma_y + \sum_{i=1}^{M} \frac{C_i}{\gamma_i}\, tanh\left(\gamma_i\, \varepsilon_{ap}\right)$. The quality of cyclic strain curve description is adequate in the case of Chaboche model within the three evolution parts. Due to the similar properties of functions $tanh(x)$ and $1 - exp(-x)$, including its derivatives, it is possible to use the same approach for parameter estimation from the monotonic even cyclic strain curves. Parameters should be determined, for example, by a nonlinear least-square method. It is useful to consider Prager's rule for the last back stress part $(\gamma_M = 0)$, the parameter influence ratcheting and mean stress relaxation effects. Therefore, we can use this approximation function for both cyclic and monotonic strain curves respectively as:

$\sigma_a = \sigma_y + \sum_{i=1}^{M-1} \frac{C_i}{\gamma_i} tanh\left(\gamma_i \varepsilon_{ap}\right) + C_M \varepsilon_{ap}$and, $\sigma_a = \sigma_y + \sum_{i=1}^{M-1} \frac{C_i}{\gamma_i}\left(1 - e^{-\gamma_i \varepsilon_p}\right) + C_M \varepsilon_p$.

When the cyclic strain curve of the investigated material is not available, it is possible to use for the calibration of the model also large saturated hysteresis loop. Based on Eq.1.13, considering tension ($\psi = 1$) and these initial values (Fig.1.7)$\alpha_0^i = -\frac{C_i}{\gamma_i}and\varepsilon_{p0} = -\varepsilon_{ap}$. We can get the expression for the upper branch of the hysteresis loop as:

$$\sigma = \sigma_y + \sum_{i=1}^{2} \frac{C_i}{\gamma_i}\left(1 - 2e^{(-\gamma_i \varepsilon_p - (-\varepsilon_{ap}))}\right) + C_3\varepsilon_p$$

.In the Chaboche model the parameter γ_M influences ratcheting (provided that the last back stress part has the lowest value of the parameter γ_i) and is chosen to be small (up to $\gamma_M = 10$). For the case of $\gamma_M = 0$ ratcheting cannot occur. However, after particular number of cycles the stabilized hysteresis loop will be formed (the Chaboche model tends to plastic shakedown) as it is clear from the graph at the Fig.1.7. For many materials such behavior does not correspond with reality and during numerical modeling, constant deformation increment can be achieved with aim of suitable choice of parameter γ_M(Chaboche and Nouailhas, 1989) $\gamma_M = \frac{\delta\varepsilon_p \cdot C_M}{2\sigma_M \cdot \Delta\varepsilon_p}$.

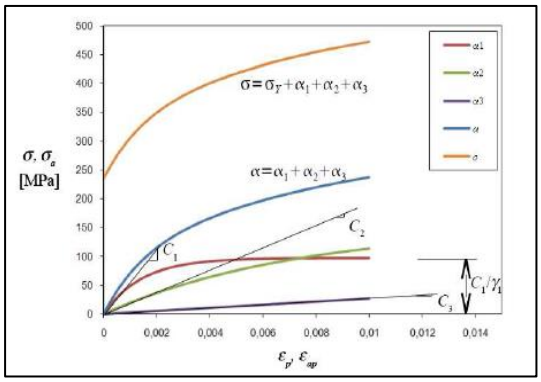

Fig1.6:*Properties of constants of Chaboche nonlinear KH model (case M=3).*

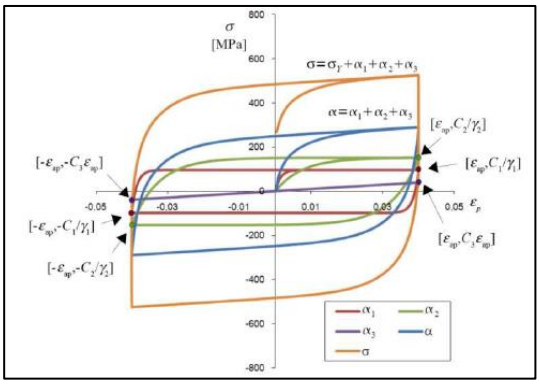

Fig1.7:*Scheme for use of the hysteresis loop to identify parameters of Chaboche model.*

Thus, with suitable choice of γ_M we get very good model for uniaxial ratcheting prediction (ratcheting with steady state only). In case of non-proportional loading the Chaboche model with three back stresses ($M = 3$) considered in Fig.1.6 and Fig.1.7 drastically over predicts ratcheting as has been shown by Bari & Hassan, 2000.

Chapter 2. Estimation of Chaboche Parameters

Following the suggestion by Chaboche, the kinematic hardening parameters are determined from strain controlled stable hysteresis loop and not from the monotonic stress-strain curve. All material parameters are determined from stable LCF hysteresis loop.

2.1 Classical approach

The value of *C1* is determined from the slope of stress-plastic strain curve of loading branch of stable hysteresis loop at cyclic yield point. Corresponding $\gamma 1$ value should be large enough that $\alpha 1$ saturates immediately. Constant slope of the stress-plastic strain curve in loading branch of stable hysteresis loop at a high strain range is *C3* and $\gamma 3$ is set to zero. *C2* and $\gamma 2$ are estimated by trial and error so that Eq.(2.1)is satisfied, $C1 > C2 > C3$ and $\gamma 1 > \gamma 2 > \gamma 3 = 0$ and represent the experimental hysteresis loop satisfactorily.

$$\frac{C1}{D1} + \frac{C2}{D2} + \sigma_0 = \sigma - \frac{C3}{2}\left[\varepsilon_p - \left(-\varepsilon_{yc}^{p}\right)\right] \tag{2.1}$$

A MATLAB program (*khparam.m*) has been developed to calculate the material parameter by the above method. The inputs to this subroutine are: true stress – true strain data, Young's Modulus, Poisson's ratio and the value of cyclic yield stress (CYS), and the location where first segment ends (*locate1*). First it is required to calculate the plastic strain, hardening stress and back stress at each point of strain data for which stress is higher than $2 * CYS$.

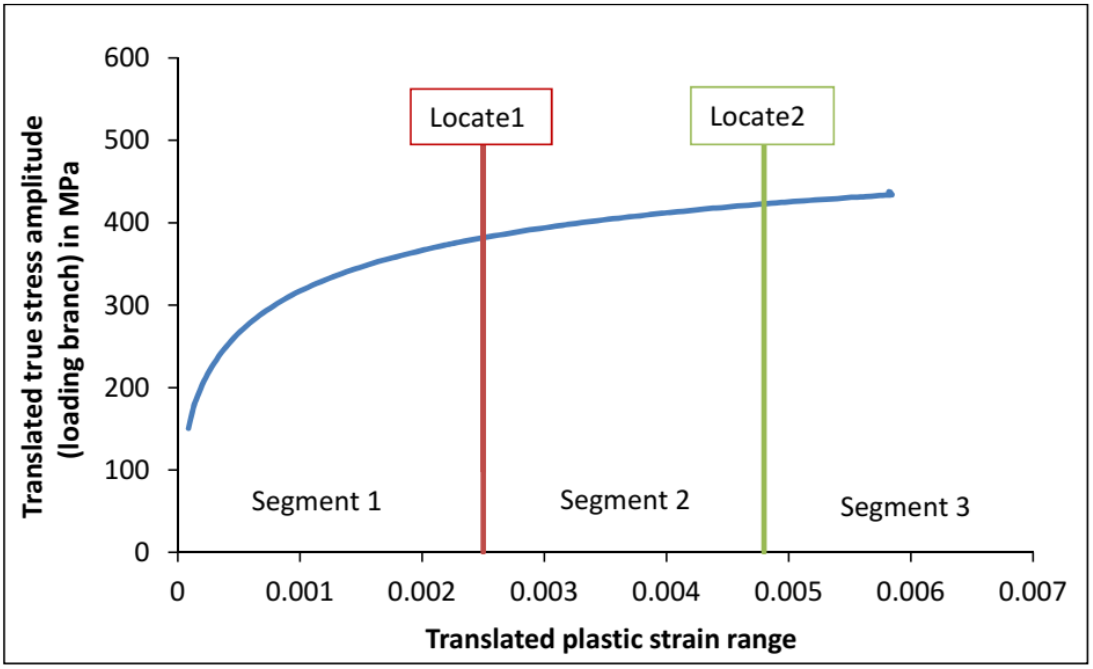

Fig.2.1 *Schemes for identification of Chaboche parameters*

In the following portion of the thesis, $\gamma 1$, $\gamma 2$, $\gamma 3$ have been referred to $D1$, $D2$, $D3$ respectively *for the convenience in coding.*

Direct calculation of C1, D1: Plastic strain at a point 'i' can be calculated as

$$plastic\_strain(i) = True\_strain(i) - \frac{True\_stress(i)}{E}$$

Hardening stress at a point 'i' is calculated as

$$Hardening\_stress(i) = \frac{True\_stress(i)}{2} - cys$$

Back stress (α) at a point 'i' is given by

$$\alpha(i) = 2 \times \frac{Hardening\_stress(i)}{3}$$

Then loading branch is divided into three segments. The strain amplitude where first segment ends, marked by *locate1* is taken as 0.0004, though its choice is somewhat arbitrary.

In the third segment there is no recovery as $D3 = 0$ so from the peak point move backward up to a point so that it fits linearly. This is ensured by the value of R-squared error not crossing 0.95. And the point up to which this condition is satisfied is marked as *locate2* which is the starting point for the third segment**.**

C1 is calculated from the slope of the line drawn taking first two points after cyclic yielding. If the index 'i' for the first two points of the hysteresis curve, be written as '1' and '2' respectively then,

$$C1 = \frac{3}{2} \times \frac{\alpha(2) - \alpha(1)}{plastic\_strain(2) - plastic\_strain(1)}$$

C3 is calculated from the slope of the line joining the first point of segment3 marked by *locate2* and last point of segment3 marked by 'k'. D1 is calculated from the value of C1, hardening modulus and the value of back stress at the point *locate1*.

$$C3 = \frac{3}{2} \times \frac{\alpha(k) - \alpha(locate2 + 1)}{plastic\_strain(k) - plastic\_strain(locate2 + 1)}$$

Hardening Modulus (H) at the point where segment1 ends i.e. locate1, is given by,

$$H(locate1) = \frac{\alpha(locate1) - \alpha(locate1 - 1)}{plastic\_strain(locate1) - plastic\_strain(locate1 - 1)}$$

$D1$ is given by,

$$D1 = \frac{\frac{2}{3} \times C1 - H(locate1)}{\alpha(locate1)}$$

And $D3$ is set to zero.

Optimization of C2 by trial and error: C2 is calculated by trial and error. The range of the C2 value can be found by lowest (at the end point of segment2) and highest (at the initial point of segment2) value of the slope of *segment2*.

So the lower and higher value of C2 is given by,

$$C2\_lo = \frac{3}{2} \times \frac{\alpha(locate2) - \alpha(locate2 - 1)}{plastic\_strain(locate2) - plastic\_strain(locate2 - 1)}$$

$$C2\_hi = \frac{3}{2} \times \frac{\alpha(locate1 + 1) - \alpha(locate1)}{plastic\_strain(locate1 + 1) - plastic\_strain(locate1)}$$

The value of $C2/D2$ ratio can be determined by solving the Eq.2.1, using the values of $C1$, $D1$, $C3$ as calculated above.

Now a value of C2 can be guessed within the range (C2_lo, C2_hi). And the value of D2 can be calculated from C2/D2 ratio. Using these values of the six parameters LCF can be simulated using Chaboche model and the resulted stress strain data can be compared with the experimental data. By manually repeating the last step better solution for the set of six parameters can be found.

2.2. Scope of optimization – sensitivity of Chaboche parameters

Thus obtained material parameters results in rudimentary simulation of plastic curvature. After through scrutiny of the experimental curve it is observed that the cyclic yield stress and location of the first segment cannot be determined deterministically from the experimentally true stress – plastic strain hysteresis loop data. In the sections below the influences of such parameters are discussed.

2.2.1 Influence of the choice of cyclic yield stress:

The value of the material parameters depends on the point where the yielding starts**,** but the value of the cyclic yield stress (CYS) cannot be chosen deterministically. As the $C1$ is calculated from the slope of the curve just after yielding, so the value of $C1$ changes with change in the value of CYS. The value of $D1$ is calculated by the above described method taking the locate1 point as 0.0004 strain amplitude for each case. $C2$, $D2$ has been solved iteratively. And the value of $C3$ is the slope of the third segment so it is same for each case. The value of the each parameter used for simulation has been tabulated in the Table 2.1.

Table 2.1: *Influence of CYS on C1, D1 and C2, D2*

CYS	C1	D1	C2	D2	C3	D3
180	616624	4391	70550	1030	16408	0
200	602321	5194	72767	1026	16408	0
220	322729	2737	72543	1587	16408	0
240	294347	3248	17835	1064	16408	0

Fig.2.2 below shows how the simulated true stress-true strain hysteresis loop varies for different choices of cyclic yield stress.

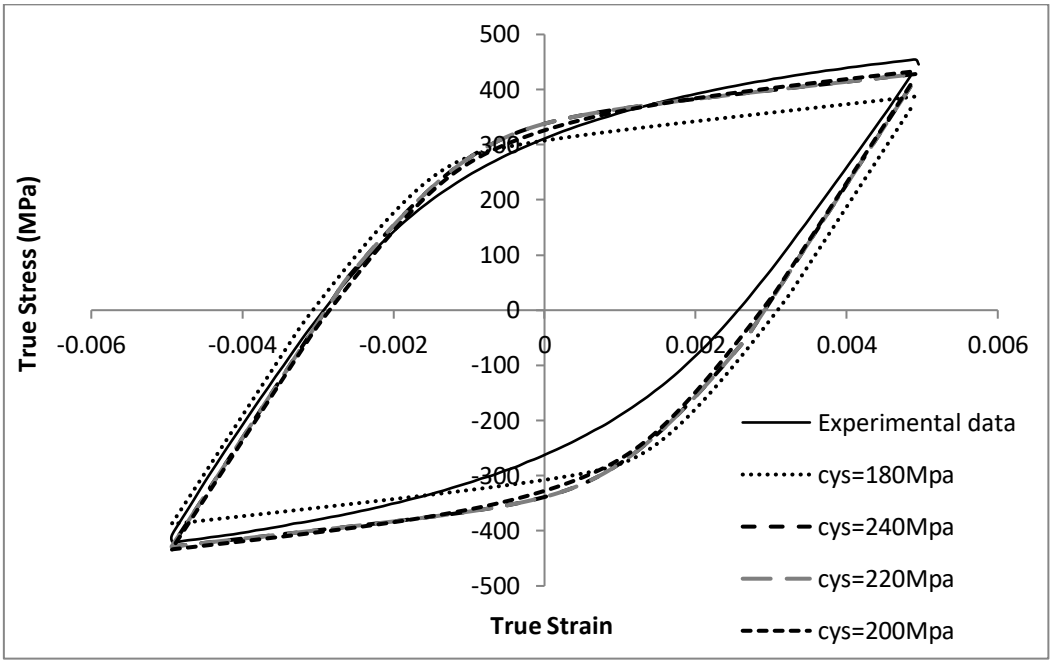

Fig.2.2: *Hysteresis loops for cyclic stress strain for various values of CYS*

2.2.2 Influence of the width of first segment

For a particular value of CYS, if we change the position where the first segment ends, the hysteresis loop also changes. The CYS has been kept fixed at $205\ MPa$ and the point locate1 has been varied. $C1$ has been calculated from initial two points after cyclic yielding in each case. So the value of $C1$ is same in each case. The value of $D1$ has been calculated by the method described above. $C2$ and $D2$ has been solved iteratively. And as $C3$ is the slope of the Third segment it is also same in each case. The values of the parameter which has been used for each simulation are tabulated in Table 2.2.

Table 2.2: *Influence of width of segment on C1, D1 and C2, D2*

CYS	Locate1	C1	D1	C2	D2	C3	D3
205	0.0002	577785	6166	109097	1248	16408	0
205	0.0005	577785	4845	61112	989	16408	0
205	0.001	577785	3852	35429	1142	16408	0
205	0.0015	577785	3404	26200	2318	16408	0

The resulted Hysteresis loop is shown below in Fig 2.3.We can observe that though there is no change in the value of C1 but as the calculation of D1 depends on the choice of segment1,So the value of D1 changes. As a result the amount of recovery for the first segment of the loop varies. And also as the C1/D1 ratio changes so to solve equation 2.1 iteratively the value of C2 and D2 also changes, so the 2nd segment of the loop also varies.

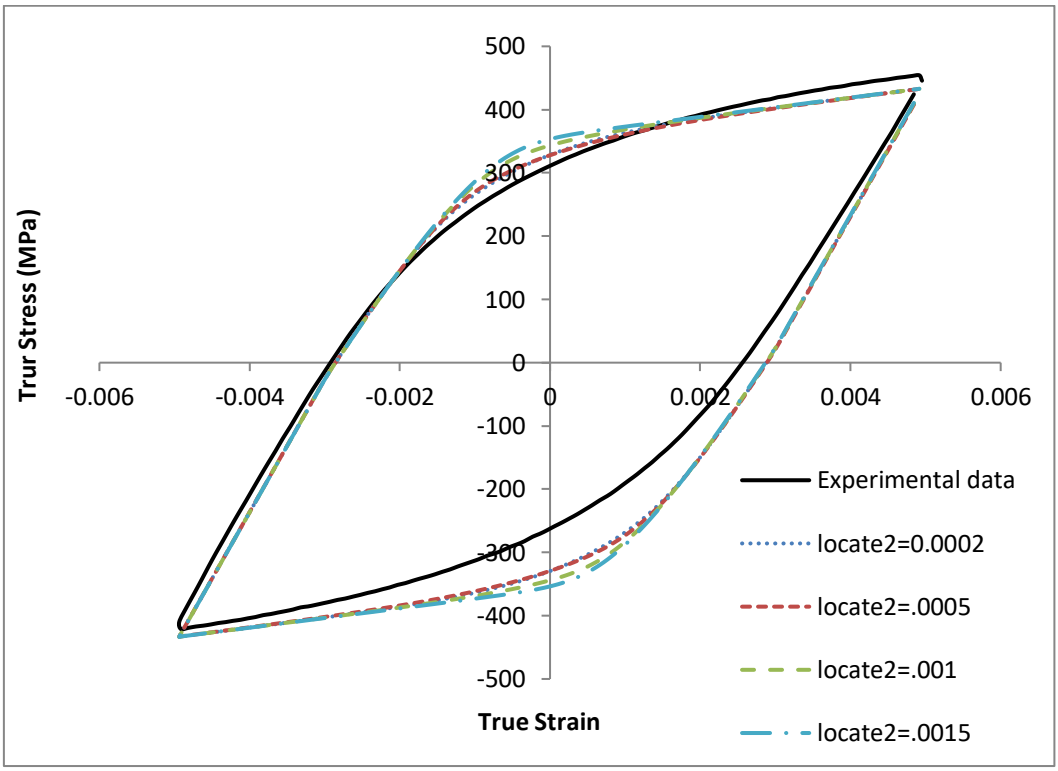

Fig.2.3: *Hysteresis loops for cyclic stress strain for various values of width of segment1*

2.2.3 Effect of C1

As previously discussed $C1$ is the slope of the initial portion of the curve which is very high, so the variation in $C1$ changes the high plasticity modulus at the onset of yielding and it stabilizes very rapidly. And with variation in $C1$ the amount of dynamic recovery for the first segment also changes. As a result the $C2/D2$ ratio changes, which, in turn affects the transient nonlinear segment of the hysteresis loop i.e. *segment2* (fig2.4).

Material models differ in the range of material properties they can describe and proportionally, in complexity of their definition. Complex material models are characterized by numerous material parameters that have to be carefully identified to follow material behavior as accurately as possible. Due to the complexity of chosen Chaboche [(J. L. Chaboche, 2008), (J. Lemaitre, J. L. Chaboche, 1990)] kinematic hardening rule, it is necessary to use complex numerical procedures to identify material parameters.

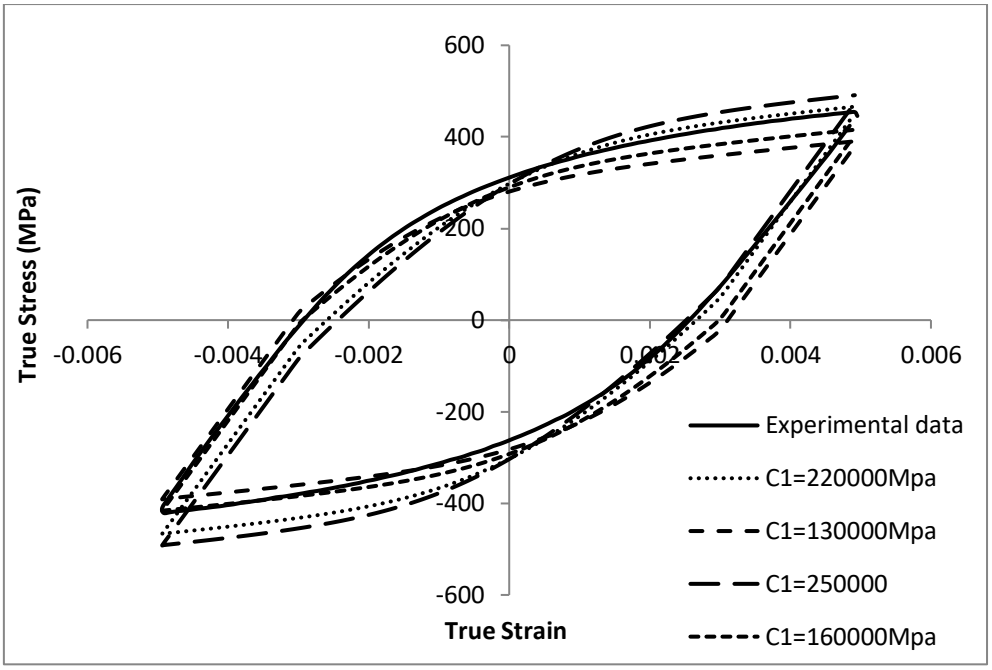

Fig2.4: *Effect of C1 on Hysteresis loop*

2.3 Objective of the work

In order to determine the Chaboche kinematic hardening parameters through optimization our objective should be focused on the choice of evolutionary algorithm and LCF simulation of Chaboche model.

2.3.1. Use of evolutionary algorithm:

Based on proposed material model and its mechanical principle, the parameters of kinematic hardening ($C1$, $D1$, $C2$, $D2$, $C3$ and $D3$) are obtained on the basis of material response in the fully reversed tensile – compressive cyclic tests, from the recorded cyclic stress – strain curves. The calculation procedure is automated by using evolutionary algorithm for material parameters identification and finite element method material behaviour simulation. The genetic algorithm based procedure consists of three main parts. The first part is system characterization, which means determination of parameters that can completely characterize the system. In the second part, forward modelling, mechanical principles and physical laws are defined to enable prediction of system behaviour. The third part is backward or inverse modelling. Inverse analysis plays an important role in problems where the cause has to be defined from the results. It consists of defining the search methods of unknown sample characteristics by observing sample's response to a probing signal. Definition of objective function represents the solution of inverse problem. The mathematical structure of the model is $\sigma = \hat{\sigma}(\varepsilon, a_i)$, which is defined by mapping function which defines the dependence among stress and strain values and the material parameter values $a_i = [C1, D1, C2, D2, C3 \text{ and } D3]$ that are considered within the chosen domain.

2.3.2 Use of standard FEM package:

Using FEM allows detailed visualization of where structures bend or twist, and indicates the distribution of stresses and displacements. FEM software provides a wide range of simulation options for controlling the complexity of both modeling and analysis of a system. Similarly, the desired level of accuracy required and associated computational time requirements can be managed simultaneously to address most engineering applications. FEM allows entire designs to be constructed, refined, and optimized before the design is manufactured. The mesh is an integral part of the model and it must be controlled carefully to give the best results. Generally the higher the number of elements in a mesh, the more accurate the solution of the discretized problem. However, there is a value at which the results converge and further mesh refinement does not increase accuracy.

ABAQUS is a suite of powerful engineering simulation program, based on the finite element method that can solve problems ranging from relatively simple linear analysis to the most challenging nonlinear simulation. Chaboche model can be simulated by FE software ABAQUS through UMAT. Fig2.5 shows a simulation of Chaboche model using ABAQUS with UMAT.

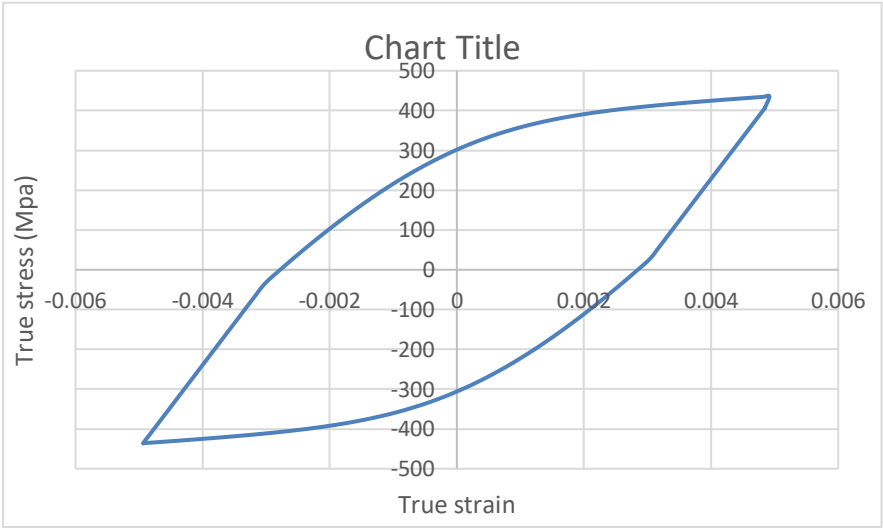

Fig2.5:simulation of low cycle fatigue using ABAQUS

2.4 Goal setting:

Based on the above objective our goal is concerned specifically to the following facts:

2.4.1 Optimization using GA:

The usage of evolutionary algorithms is proposed because of their advantageous characteristics, mainly considering insensitivity to errors in measured data, reliability in

achieving convergence to accurate results, improbability for convergence to local minima and it's robustness regarding the choice of objective function [(T. Furukawa, G. Yagawa, 1997), (X. T. Feng, C. Yang, 2001)]. Genetic algorithm is stochastic search method for obtaining good approximate solutions for complex problems (M. Franulovic, R. Basan, I. Prebil, 2009). It is based on mechanisms of natural evolution and genetic principles. The genetic algorithm creates a population of solutions and applies genetic operators, such as scaling, selection, mutation and crossover to evolve the solutions in order to find the best ones. The proper evolution of population is assured by selection of adequate genetic operators in order to achieve fast convergence to global optima.

2.4.2 Selection of proper objective function:

One of the main premises in genetic algorithm application for parameter identification is the choice of objective function for inverse problem solution. There are numerous published papers that suggest different objective functions for the problem solution. In order to evaluate these suggestions and the influence of objective function on simulation of material behavior by parameter identification with genetic algorithm usage, the most common ones are investigated [(T. Furukawa, T. Sugata, S. Yoshimura, 2002), (R. Fedele, M. Filippini, G. Maier, 2005), (D. Szeliga, J. Gawad, M. Pietrzyk, 2004)], and also their modified versions that are implemented. Scaling of population is based on the fitness values of the individuals, which is the solution of chosen objective function .In general

$$f = \sum_{i=1}^{n} \left[\frac{y_i^* - \hat{y}(x_i^*; \text{parameters})}{y_i^*} \right]^2$$

Where asterisk * refers to experimental value, while mark ^ refers to value calculated by using set of parameters. The chosen objective functions used for comparison in this research are taken in the form published by some authors and also in modified form of each of them as shown in Table 2.3

Table 2.3: List of objective function for material parameters identification which have been used by various researchers

Source	Function
T. Furukawa, T. Sugata, S. Yoshimura,2002	$f = \sum_{i=1}^{n} w_i[\sigma_i^* - \hat{\sigma}(\varepsilon_i^*; a)]^2 \ ; \ w_i = 100$
R. Fedele, M. Filippini, G. Maier,2005	$f = \sum_{i=1}^{n} \left[\frac{\sigma_i^* - \hat{\sigma}(x_i^*; a)}{\sigma_i^*} \right]^2$
D. Szeliga, J. Gawad, M. Pietrzyk,2004	$f = \sqrt{\frac{1}{n} \sum_{i=1}^{n} \left[\frac{\sigma_i^* - \hat{\sigma}(x_i^*; a)}{\sigma_i^*} \right]^2}$

2.4.3 Bridging the gap between coding environment and FE package:

MATLAB platform has been used for preprocessing of the data, and computer implementation of GA whereas for Finite element simulation ABAQUS has been used. In need for exhaustive searching by GA , at each loop it is required to compare the simulated data with the experimental data. So MATLAB has to call ABAQUS and update the current set of values of the Chaboche parameters and extract the simulation results in an atomized way. And as the two software environment is not same in nature so it is a challenge to link MATLAB with ABAQUS.

2.5 Benchmarking

Parameter optimization problems start with experimentation and data extraction, followed by preparing the data for further processing. The steps can be classified as:

1) **Experimentation:** LCF experimentation for a single strain amplitude (0.5 %) for the material, Identification of the material behaviours, data collection and extraction of saturated loop data where modelling of the material behaviour only by kinematic hardening is justified.

2) **Preprocessing:** from the saturated cyclic true stress – plastic strain loop data, the strain increments are identified and a step time – amplitude curve is generated for FE simulations. Again from the data, only the loading branch is collected for Chaboche parameter extraction.

3) **Coding:** This is the main focus of the present work. The coding is done for three different purposes in this work: i) the main and auxiliary optimization routines in MATLAB, ii) MATLAB routines those provides the classical framework for the material parameter identification, and iii) the communication routines in PYTHON. The communication routines built the bridge between MATLAB and ABAQUS CAE environment. The updated simulation parameters are plugged into ABAQUS and simulated stress-strain data at precise location and at accurate moments are extracted out by these routines.

   Another auxiliary routine is used in this work, which is the user defined material subroutine (UMAT) for Chaboche model written in FORTRAN.

The main optimization routine is chosen to be Genetic Algorithm (GA) to avoid the dilemmas like the vibration in the solution, diverge, and local optima. The use of GA is significantly promising for complex optimization.

Chapter 3. Material and Experimental Procedure

3.1 The Material

The 20MnMoNi55 low alloy carbon steel is used in reactor pressure vessels in nuclear power plants where the operating temperature of this material is $300°C$.The pressure vessel and the primary heat transport piping of Indian PHWR nuclear power plants are designed and operated on the basis of '*leak before break*' (LBB) concept. In order to implement this LBB concept in the design of pressure vessels it is important to understand the fracture toughness behavior of the material in its operating conditions. The typical chemical composition of the present material (wt. %) is: C-0.21%, Si-0.24%, Mn-1.48%, Cr-0.20%, Ni- 0.80%, Mo-0.52%,V-0.02%, Cu-0.07%, As-0.02%, Al-0.015%,Sn-0.005%, P-0.008%, S-0.005%.

The material chiefly consists of 0.2% Carbon with 1.25% Manganese, 0.5% Molybdenum, 0.6% Nickel with small quantity of Chromium, Silicon and Sulphur. From metallurgical point of view, increase of material strength may influence on the other properties such as toughness, corrosion resistance and may also affect the weldability. So good mechanical and metallurgical properties are required to withstand the internal pressure and prevent unexpected failure during the service life. The particular material 20MnMoNi55 steel has been the subject of extensive research work recently (M. S. E1-Fadaly, T.A. E1-Sarrage, A.M. Eleiche, W. Dahl, 1995). The typical microstructure of 20MnMoNi55 steel as shown in fig.3.1 this microstructure consists of Bainite (volume fraction 35%) and Ferrite phases. Bainite is randomly oriented in Ferrite matrix, which gives more toughness. The Ferrite gives ductility and Bainite gives strength to the investigated steel.

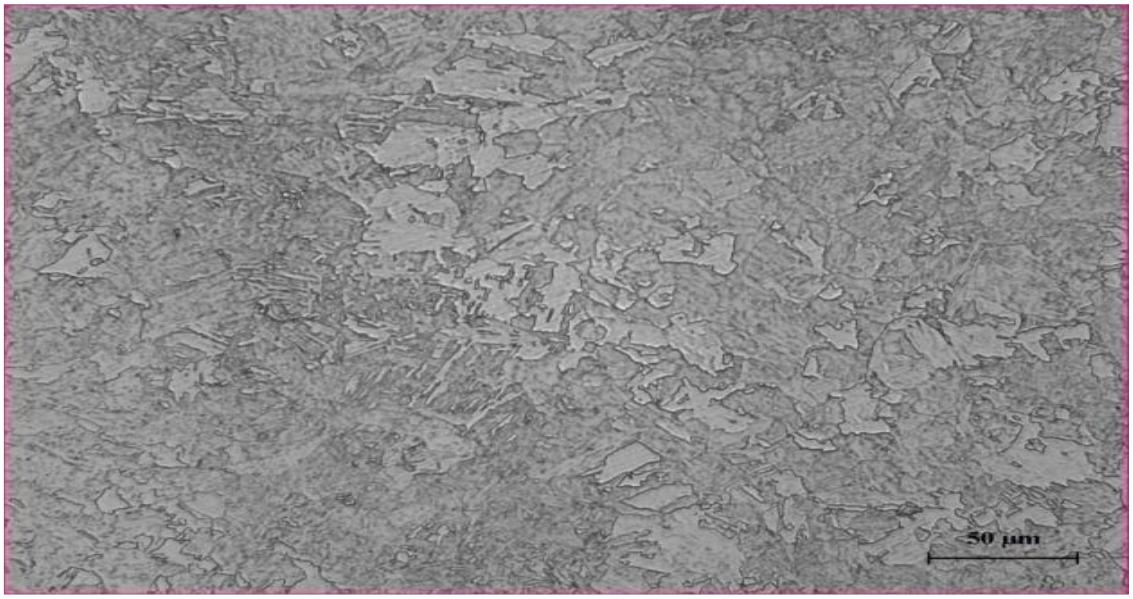

Fig 3.1: *Typical optical microstructures of the investigated steel in L-T direction*

3.2 Tensile tests

Uniaxial monotonic (tensile) tests are conducted for basic material properties. Tensile tests are performed according to ASTM E8M. Smooth round specimen with diameter 6 mm and gauge length 30 mm ($5D$) are used. A brief account of the tests are presented in table 3.1:

Table 3.1: *Overview of the monotonic tests.*

	Details	**Specification**	**Standard/ Grade**	**Maker**	**Remarks**
Testing Machine	Servo-Hydraulic Universal Testing Machine	100kN Grip Capacity, 8800 Controller		Instron	Blue Hill v3.0 software used
Measuring Instrument	Vernier Caliper	0 – 200mm L.C. – 0.02		Mitutoyo	
	Extensometer	Static, 25 ± 5mm		Instron	
Test Specimen	20MnMoNi55 RPV steel, round, threaded	ϕ 6 mm, GL 30 mm, M10x25 coarse thread	ASTM E8M	Local Vendor	Dimensions are in 'mm'
Test Procedure	Tests are done in Displacement Controlled mode, at room temp. (300K), and quasistatic Strain rate (10^{-3} per second)		ASTM E8M	As per ASTM	Current strain rate and temperature do not produce any rate effects

Representative tensile stress – tensile strain curve for 20MnMoNi55 low alloy RPV steel is shown in figure 3.2 below.

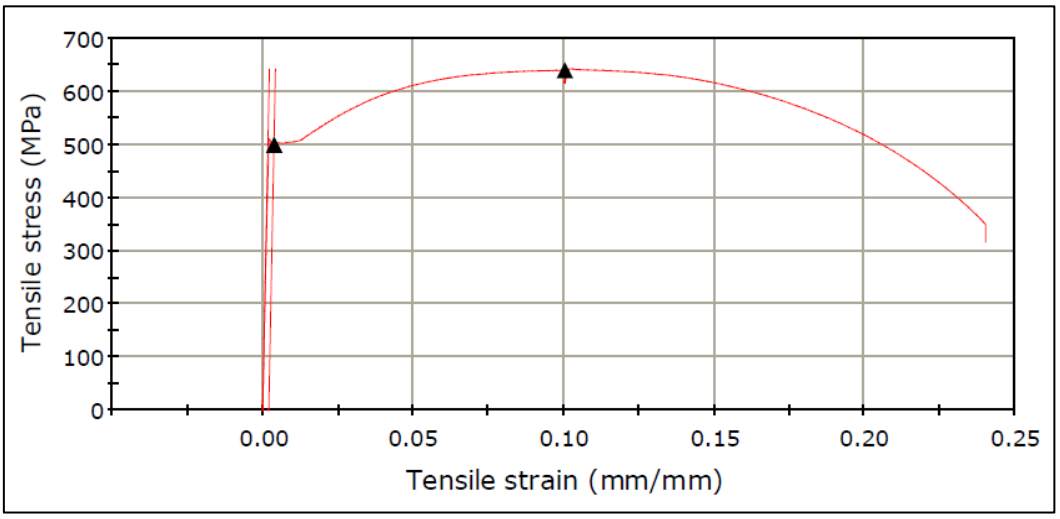

Fig3.2: *Tensile stress vs tensile strain curve*

Typical tensile properties of the material is Young's modulus (tensile strain 0.01 % - 0.1 %): 209561.56187 MPa, Tensile stress at Yield (Offset 0.2 %): 499.95732 MPa, Tensile Strength: 642.51389 MPa, Percentage Elongation: 24.252 %. For numerical simulations, the Poisson's ratio is taken to be 0.3 typically.

3.3 Uniaxial low cycle fatigue (LCF) tests:

As per ASTM 606M, standard round non-threaded specimens of 8mm diameter and 20mm gauge length (> 2D) are fabricated from the pipe stock available with their axes parallel to the pipe axis. The specimen geometry is as shown in figure 3.3a. All tests are carried out in strain controlled mode at a strain rate of 10^{-3} s^{-1} and accordingly the displacement rates and the data extraction frequencies (200 pts. per cycle) are adjusted to achieve constant strain rate and accurate results without losing valuable information as far as possible.

Similarly like tensile tests, uniaxial LCF experiments are also carried out using above mentioned servo-hydraulic testing machine in the laboratory environment (27°C, 50% Relative Humidity). A close-up of the experimental setup is shown in figure 3.3b.

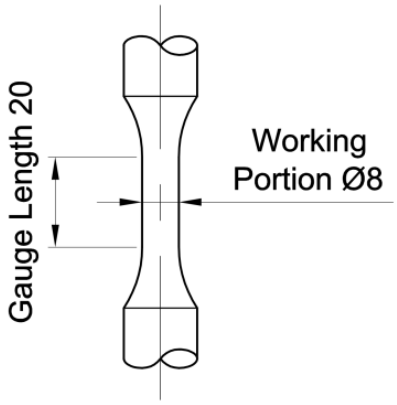

Fig3.3a: *Uniaxial specimen geometry (dimensions are in 'mm').*

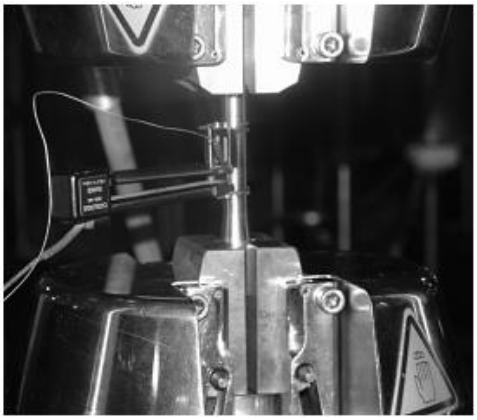

Fig3.3b: *Uniaxial testing system (INSTRON 8800).*

A 12.5 mm gauge length extensometer (INSTRON make) with ±5 mm travel is to be used to measure the strain during LCF tests. Tests are continued till failure and stress-strain data acquired throughout the test so as to obtain ~200 data points in each stress cycle for cyclic tests. Tests are conducted under software (Wave Matrix) control using a computer interfaced to the INSTRON 8800 control system of the testing machine and capture data automatically.

Representative true stress – true strain hysteresis loop at saturated cycle for the material is shown below in figure 3.4.

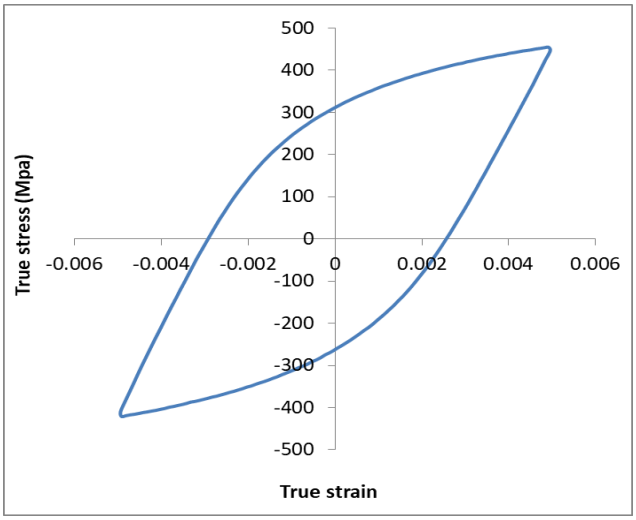

Fig3.4:*Typical saturated (200th) cycle true stress vs. true strain experimental data for 0.5 % strain amplitude for 20MnMoNi55 RPV steel at room temperature and quasi-static strain-rate.*

Chapter 4. GA based optimization of Chaboche parameters

4.1 Overview of Genetic Algorithm

The genetic algorithm (GA) is an optimization and search technique based on the principles of evolution and natural selection. The genetic algorithm can be applied to find optimal solution and to solve equations.A GA allows a population composed of many individuals to evolve under specified selection rules to a state that maximizes the "fitness" (i.e., minimizes the objective function). A path through the components of the GA is shown in flowchart in Fig.4.1

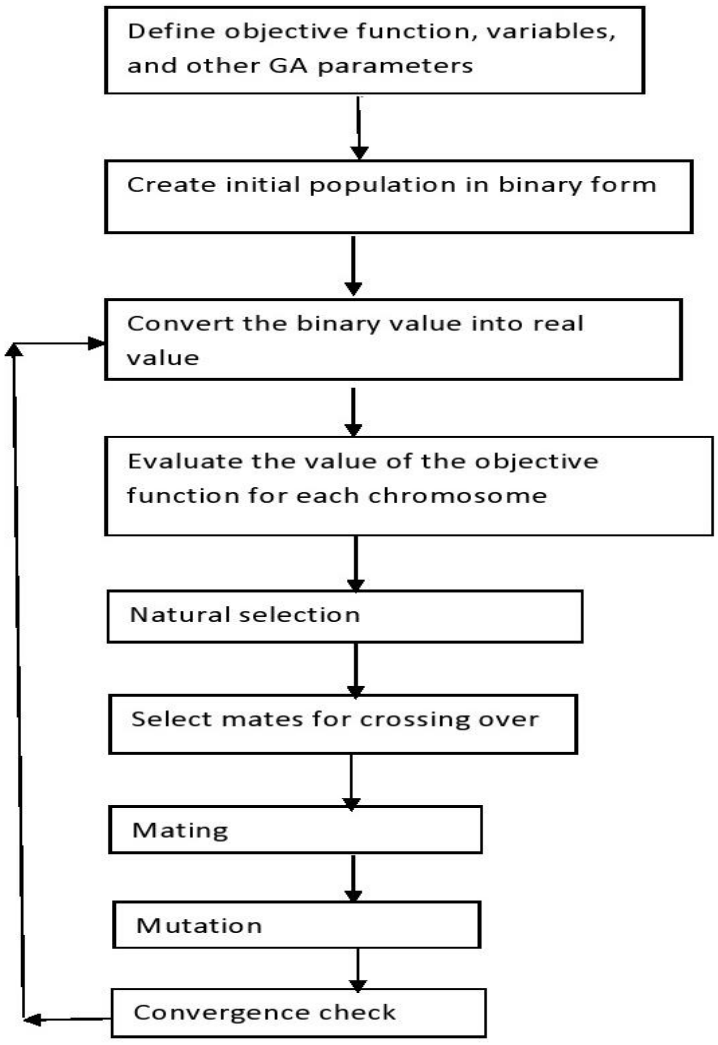

Fig.4.1: *Flowchart of a binary genetic algorithm*

4.1.1 Selecting the Variables and the Cost Function

The GA begins by defining a chromosome or an array of variable values to be optimized. If the chromosome has N_{var}variables (an N_{var}-dimensional optimization problem) given by $p1$, $p2$ … p_{var} then the chromosome is written as an N_{var} element row vector.

$$Chromosome = [p1, p2, p3 \ldots pvar]$$

An objective function generates an output from a set of input variables (a chromosome) .The object is to modify the output in some desirable fashion by finding the appropriate values for the input variables. Each chromosome has a cost found by evaluating the objective function, f, at $p1$, $p2$, . . . ,pN_{var}

$$Cost = f\ (Chromosome) = f(p1, p2, \ldots . pNvar)$$

4.1.2 The Population

The GA starts with a group of chromosomes known as the population. If the population size is N_{pop} then the population has N_{pop} chromosomes and is an $N_{pop} \times N_{bits}$ matrix filled with random ones and zeros, where N_{bits} is the no of bits required to represent a variable. It has been recognised that if the initial population to the GA is good, then the algorithm has a better possibility of finding a good solution [(E. K. Burke, S. Gustafson, and G. Kendall, 2004), (E. Zitzler, K. Deb, and L. Thiele, 2000)]. If the similarity of the population is too high, then the convergence speed is low. The initialization of the individuals of the population should be as uniformly distributed as possible but it is hard to achieve because initialization is random. The uniform initialization gives the GA a better performance because there is an individual in each area of the search space (Chou C.H. and Chen J.N, 2000).

4.1.3 Variable Encoding and Decoding

Since the variable values are represented in binary, there must be a way of converting continuous values into binary, and vice-versa. The mathematical formulas for the binary encoding and decoding of the nth variable, p_n, are given as follows:

For encoding,

$$P_{norm} = \frac{P_n - P_{lo}}{P_{hi} - P_{lo}}$$

$$gene\{m\} = round\{P_{norm} - 2^{-m} - \sum_{P=1}^{m-1} gene[p]2^{-p}\}$$

For decoding,

$$P_{quant} = \sum_{m=1}^{N_{gene}} gene[m]2^{-m} + 2^{-(M+1)}$$

$$q_n = P_{quant}(P_{hi} - P_{lo}) + P_{lo}$$

In each case, P_{norm}=normalized variable,$0 \leq P_{norm} \leq 1$, P_{lo}=smallest variable value, P_{hi}=highest variable value, gene[m]=binary version of P_n,round{.}=round to nearest integer, P_{quant}=quantized version of P_{norm},q_n=quantized version of P_n

The quantized value of the gene or variable is mathematically found by multiplying the vector containing the bits by a vector containing the quantization levels:

$$q_n = gene\ X\ Q^T$$

Where, $gene = [b_1, b_2 \ldots b_{Ngene}]$, N_{gene}= number bits in a gene, b_n= binary bit = 1 or 0, Q = quantization vector = $[2^{-1}, 2^{-2} \ldots 2^{Ngene}]$, Q^T= transpose of Q.

Thus if a continuous variable is to be represented with high accuracy, we need to use alarge value of N_{gene}in its binary representation. In fact, the number of binary digits needed(N_{gene}) to represent a continuous variable in steps (accuracy) of Δx can be computed fromthe relation

$$2^{Ngene} > \frac{P_{hi} - P_{lo}}{\Delta x} + 1$$

4.1.4 Selection

Selection is the component which guides the algorithm to the solution bypreferring individuals with high fitness over low-fitted ones. It can be adeterministic operation, but in most implementations it has random components. There are varieties of selection methods. Some of them are described below.

Roulette wheel selection: In this method for a minimization problem the probabilities assigned to the chromosomes are inversely proportional to their cost. A chromosome with the lowest cost has the greatest probability of being selected, while the chromosome with the highest cost has the lowest probability of selection. A random number determines which chromosome is selected. A normalized cost is calculated for each chromosome. Then for each chromosome cumulative probability is calculated. And the range in which the generated random no falls, the chromosome corresponding to that range is selected. The detailed algorithm of this selection scheme has been discussed in section 3.2.3. This approach tends to weight the top chromosome more when there is a large spread in the cost between the top and bottom chromosome. On the other hand, it tends to weight the chromosomes evenly when all the chromosomes have approximately the same cost. Instead of weighting based on actual cost we can also weight the chromosomes based on their rank obtained after sorting the population according to their cost. In this case the probability of selection for a particular row of population matrix is same in each iteration, so small populations have a high probability of selecting the same chromosome.

In the beginning, the potentially good individuals sometimes fill the population too fast which can lead to premature convergence into local maxima or minima. On the other

hand, refinement in the end phase can be slow since the individuals have similar fitness values. These problems can be overcome by taking the rank of the fitness values as the basis for selection instead of the values themselves. So choice of selection scheme is problem dependent.

Tournament selection: Another approach that closely mimics mating competition in nature is to randomly pick a small subset of chromosomes(two or three) from the population, and the chromosome with the lowest cost in this subset is selected for the new population. The Tournament selection works best for larger population sizes because sorting becomes time consuming for large populations. Thisselection scheme is also applicable when the fitness function is given in implicit form, i.e. when we only have a comparison relation which determines which of two given individuals is better.

Algorithm:

In this roulette wheel selection scheme with cost based weighting has been used. The roulette wheel selection scheme can be implemented as follows:

1. Evaluate the fitness, f_i, of each individual in the population.

2. Compute the probability (slot size), p_i, of selecting each member of the population:

$$p_i = f_i / \sum_{j=1}^{n} f_i$$

Where n is the population size.

3. Calculate the cumulative probability, q_i, for each individual:

$$q_i = \sum_{j=1}^{i} p_j.$$

4. Generate a uniform random number, r $\in$(0, 1].

5. If $r<q_1$ then select the first chromosome, x_1, else select the individual xi such that $q_{i-1}<r \leq q_i$

6. Repeat steps 4–5 n times to create n candidates in the mating pool.

4.1.5 Cross-over

The purpose of crossover is to create new strings by exchanging information among strings of the mating pool.Mating is the creation of one or more offspring from the parents selected in the pairing process. The genetic makeup of the population is limited by the current members of the population. One method (termed single point crossover) is to choose pairs of individuals promoted by the selection operator, randomly choose a

single locus (point) within the binary strings and swap all the information (digits) to the right of this locus between the two individuals as demonstrated in Fig.4.2.

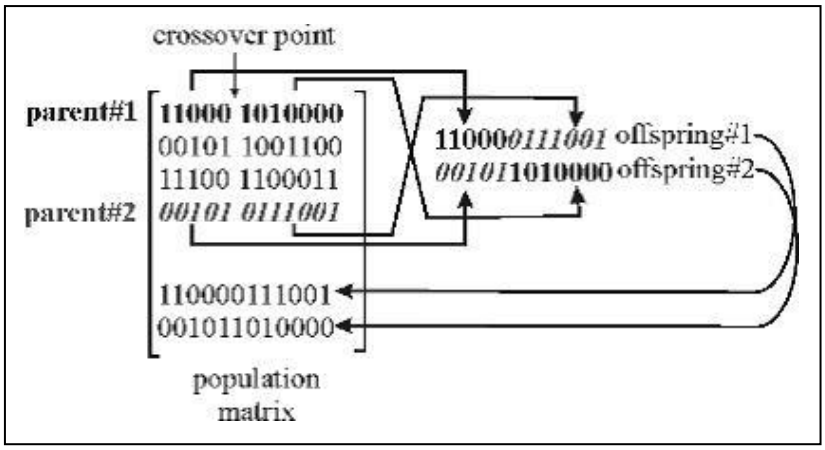

Fig4.2: *Schematic representation of Cross-over.*

Since the crossover operator combines substrings from parent strings (which have good fitness values), the resulting child strings created are expected to have better fitness values provided an appropriate (suitable) crossover site is selected. However, the suitable or appropriate crossover site is not known before hand. Hence the crossover site is usually chosen randomly. The child strings generated using a random crossover site may or may not be as good or better than their parent strings in terms of their fitness values. If they are good or better than their parents, they will contribute to faster improvement of the average fitness value of the new population. On the other hand, if the child strings created are worse than their parent strings, it should not be of much concern to the success of the GAs because the bad child strings will not survive very long as they are less likely to be selected in the next reproduction stage (because of the survival-of-the-fittest strategy used).One-point crossover is a simple and often-used method for GAs which operates on binary strings. For other problems or different coding, other crossover methods can be useful or even necessary. We mention just a small collection of them, for more details see [(GEYER-SCHULZ, A, 1996), (GOLDBERG, D. E, 1989)].

N-point crossover: Instead of only one, N breaking points are chosen randomly. Every second section is swapped. Among this class, two point crossover is particularly important

Segmented crossover: Similar to N-point crossover with the difference that the number of breaking points can vary.

Uniform crossover: For each position, it is decided randomly if the positions are swapped.

Shuffle crossover: First a randomly chosen permutation is applied to the two parents, then N-point crossover is applied to the shuffled parents, finally, the shuffled children are transformed back with the inverse permutation.

In this case single point cross-over have been used for mating purpose.

Algorithm:

The steps of a single point cross-over are given below.

i. First the index of the individual is generated randomly who will participate in mating.

ii. For each pair of mating a random cross-over point is randomly selected in between the first and last bit of the parent string.

iii. First, *parent*1 passes its binary code to the left of that crossover point to *offspring*1. In a like manner, *parent*2 passes its binary code to the left of the same crossover point to *offspring*2. Next, the binary code to the right of the crossover point of *parent*1 goes to *offspring*2 and *parent*2 passes its code to *offspring*1. Consequently the offspring contain portions of the binary codes of both parents.

4.1.6 Mutation

Random mutations alter a certain percentage of the bits in the list of chromosomes. Mutation is the second way a GA explores a cost surface. It can introduce traits not in the original population and keeps the GA from converging too fast before sampling the entire cost surface. A single point mutation changes a 1 to a 0, and vice-versa with probability 'pm'. Mutation points are randomly selected from the N_{pop}XN_{bits}total number of bits in the population matrix. Increasing the number of mutations increases the algorithm's freedom to search outside the current region of variable space though pmshould be rather low in order to avoid that the GA behaves chaotically like a random search. Again, similar to the case of crossover, the choice of the appropriate mutation technique depends on the coding and the problem itself. There are a few alternatives, more details can be found in (GEYER-SCHULZ, A, 1996) and (GOLDBERG, D. E, 1989)again.

Inversion of single bits: With probability 'pm', one randomly chosen bit is negated.

Bitwise inversion: The whole string is inverted bit by bit with probability 'pm'.

Random selection: With probability 'pm', the string is replaced by a randomly chosen one.

Inversion of single bits has been used here for mutation purpose

Algorithm:

Mutation also simulates biologic evolution mechanism. An algorithm for mutation operation is given below

i. For the individual to mutate, randomly choose the point to mutate which means the bit of the individual encoded binary string.

ii. Change 0 to 1 and change 1 to 0, with a probability of mutation, 'pm'. For every individual, a number of probabilities of mutation are randomly given by the computer. If the giver number is not greater than pm, the individual mutates, otherwise mutation doesn't occur.

4.1.7 Main programming

Following the above overview of the algorithm for the main program is given below:

Step I First a population is created using the encoding function.

Step II Then the binary value of the variables is converted to decimal value. And the objective function is evaluated for each chromosome of the population.

Step IV Then the best solution of current generation is identified.

Step V The generation counter is initiated.

Step VI New population is created by cross over operation using the function '*cross_over'*.

Step VII Then mutation operation is done by using the function '*mutation*'.

Step VIII The new population is reevaluated for cost.

Step IX The best solution of the current generation is compared with the best solution of the previous generation and if the later one is better, it replaces the earlier else it remains unchanged. And also the worst solution of each generation is replaced with the best solution available at that time.

Step X Iteration stops when the maximum no of iteration is reached or a specified minimum allowable error is attained.

Step X Finally the best solution and corresponding set of variables are extracted using the function result.

4.2 Preprocessing of Data before calling main programme

This MATLAB code.'*preprocessor.m*'.is used for orientation of experimental data and creating loading amplitude .The data is oriented so that it can be readily compared with the simulated data. Loading amplitude is created to give as an input to the Abacus FE package. Input of this module are Young's modulus, Poisson ratio and the lowest and highest value of cyclic yield stress. Next it identifies and segregate the loading branch from the raw data

4.3 LCF modeling and simulation in ABAQUS

Uniaxial cyclic plastic deformations are simulated in ABAQUSCAE (v6.8) commercial finite element platform. Only one quarter of the working (gauge length) portion of the

actual specimenismodelled considering axisymmetric conditions. The specimen is discretized adopting structural meshing with total 154 nodes. 80 linear hexahedral (8-noded, C3D8) elements are used. The linear elements have linear shape functions and enabled for full integration (on 8 integration points). Maintaining the symmetry, displacement boundary conditions are imposed according to the strain amplitudes using balanced triangular amplitude function with time. The amplitude function is obtained from the experimental data points fitting them against proportional virtual time increment.

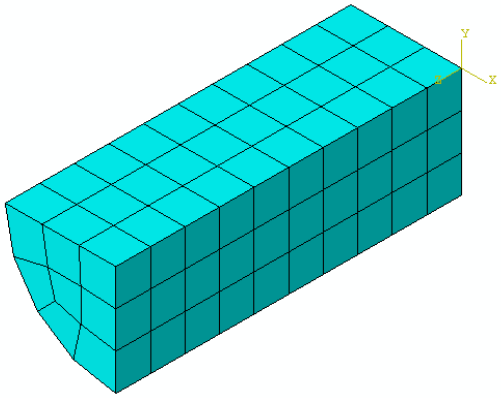

Fig. 4.3a:*Discretized specimen*

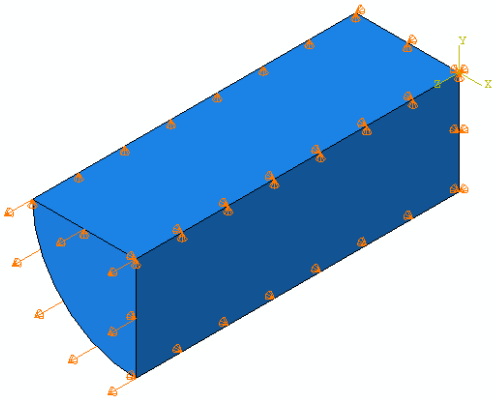

Fig.4.3b:*Axisymmetric loading arrangement*

The material model is incorporated through user material subroutine (UMAT), though the required material parameters are inserted into the ABAQUS material module. The iterative solver for the equivalent plastic strain increment and the overall integration schemes, as discussed in the previous chapter, are chosen carefully. The details of the integration scheme and the material subroutine can be found in the Annexure III.

4.4 Linking of MATLAB with ABAQUS

The ABAQUS is called by MATLAB routines through WINDOWS operating system's DOS interface as it is usually done in the ABAQUS COMMANDS (no GUI) window. But before that, necessary update information are collected from MATLAB '*ga3obj.m*' routine and saved into the ABAQUS model database (*chaboche1.mdb*) through MATLAB script '*femsol.m*'. When the model database file (*chaboche1.mdb*) is run through PYTHON, in the ABAQUS NO GUI COMMAND interface, it saves all necessary updates into ABAQUS model database file.

Then in the '*femsol.m*' ABAQUS STANDARD solver is invokedthrough ABAQUS NO GUI COMMAND interface and ABAQUS simulates the LCF experiment with the updated parameters. After the simulation is done '*femsol.m*' calls another PYTHON script '*odbout.*py' in the ABAQUS VIEWER NO GUI interface for extracting necessary field outputs at precise locations. The outputs are mainly true stress and true strain loop data along with two marker and flag operator to select only plastic regimes of the loop. Thus obtained simulated true stress data at similar strain points as in the experimental result are then compared and the differences and cumulative error are calculated.

To run this entire sequence in an automated fashion, the DOS windows are closed after specific operation which is accomplished by introducing '/c' flag in the ABAQUS NO GUI COMMAND prompt.

4.5 The entire optimization sequence

To obey the constraints of the Chaboche model, a scheme of sequential GA (or nested GA) has been planned. The requirement and execution of such planning has been described below in detail.

The value of cyclic yield stress cannot be identified deterministically. So first a population of CYS is created under GA1.C3 can be determined by linear fitting of the third segment. From the maximum strain point the point up to which the linear fits hold well is the point locate2.

Now the actual width of segment1 is not precisely defined, rather its range can be identified from the fig 3.3. The starting point of segment1 is selected as the point cyclic yielding. And the last point of segment1 i.e. locate1 can be anywhere between the point of cyclic yielding and locate2, so to identify segment1 we can create a range for actual position of the point locate1, only after creating a population of CYS by GA1, which can be given as an input to another GA (GA2) to find the best position of locate1 corresponding to a particular value of CYS. This is also the reason why GA2 is called inside GA1.

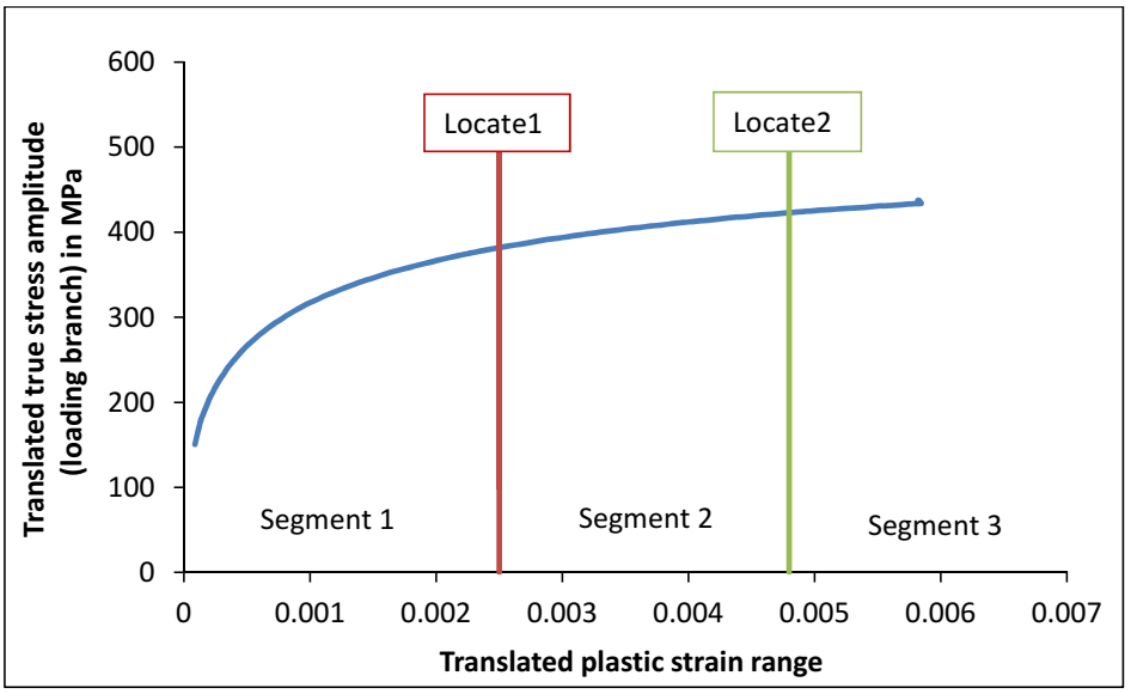

Fig.4.4: *Schemes for identification of Chaboche parameters*

Now according to the section 1.3.1 the following facts regarding the upper and lower limit of C1, C2 can be observed.

Higher limit of C1: slope of the hysteresis curve just after the point of cyclic yielding.

Lower limit of C1: slope of the hysteresis curve taking the two points locate1 and the point just before it.

Higher limit of C2: slope of the hysteresis curve taking the two points locate1 and the point just after it.

Lower limit of C2: slope of the hysteresis curve taking the two points locate2 and the point just before it.

So it is clear from the above considerations that the range of C1, C2 depends on the choice of CYS, locate1 and locate2 so we call the 3rd GA for each iteration of GA2 to find the best value of C1, C2 for a particular value of CYS and locate1.

The population of C1, C2 is created under GA3. After that the value of D1, D2 is calculated deterministically as described in section 2.1 for each value of CYS, locate1, C1, C2, C3, D3. Now the complete set of Chaboche material parameters is available to run the simulation in ABAQUS, so that simulated stress strain data can be extracted. Now a suitable comparison method has to be used for comparing the experimental and simulated data by GA3.

Definition of the objective function for GA3

The **root-mean-square error (RMSE)** (or sometimes **root-mean-squared error**) between the stress value generated by simulation and experiment for each of the 200 points of strain values obtained from experimental result has been used as the objective function by GA3 which has to be minimized. RMSE is a frequently used measure of the differences between values (sample or population values) predicted by a model or an estimator and the values observed. The RMSD represents the square root of the second sample moment of the differences between predicted values and observed values or the quadratic mean of these differences. These deviations are called *residuals* when the calculations are performed over the data sample that was used for estimation and are called *errors* (or prediction errors) when computed out-of-sample. The RMSD serves to aggregate the magnitudes of the errors in predictions for various times into a single measure of predictive power. RMSD is a measure of accuracy, to compare forecasting errors of different models for a particular dataset and not between datasets, as it is scale-dependent.[1]

RMSD is always non-negative, and a value of 0 (almost never achieved in practice) would indicate a perfect fit to the data. In general, a lower RMSD is better than a higher one. However, comparisons across different types of data would be invalid because the measure is dependent on the scale of the numbers used.

RMSD is the square root of the average of squared errors. The effect of each error on RMSD is proportional to the size of the squared error; thus larger errors have a

disproportionately large effect on RMSD. Consequently, RMSD is sensitive to outliers (Willmott, Cort; Matsuura, Kenji, 2006; Pontius,Robert; Thontteh, Olufunmilayo; Chen, Hao; 2008)

$$RMSE = \sqrt{\frac{\sum_{t=1}^{T}(\hat{\sigma} - \sigma)^2}{T}}$$

Where $\hat{\sigma}$ is the simulated value of the stress for a particular strain and σ is the experimental value of the stress for the same strain value. 'T' is the total no of strain points which in this case is '200'

The whole process of the above described method is given below in step by step manner and also fig 4.5 shows the flowchart.

1. GA1 creates a population of CYS then it calls '*khparam3.m*' to calculate C3 and the location of the initial point of 3rd segment.

2. Call *khparam4* to calculate the range locate1.

3. The above output is given as a input to GA2 for finding the best value of locate1 corresponding to a particular value of CYS. GA2 first creates the population of locate1. Then it calculates range of C1, C2 by calling khparam5 for each value of locate1.

4. GA3 creates population of C1, C2 to find the best value of C1, C2 for a particular value of CYS and locate1.

5. *khparam6* to calculate the value of D1, D2.

6. Update the above calculated material parameters to the model database file of ABAQUS and submit the job to the ABAQUS to get the simulated value corresponding to a particular set of CYS and six material parameters.

7. Then the stress values for the given strains are extracted from the output database of the ABAQUS compares the experimental results and simulated results and evaluates the objective function and find the best value of C1,C2 for a particular CYS and locate1.

9. And the best value of C1, C2 corresponding to lowest least square error for each value of locate1 is passed to GA2.

10.Then GA2 find the best locate1 corresponding to lowest value of least square error and sent that to GA1 which contains best value of locate1,C1,C2 for each value of CYS.

11. GA1 finds the best value of CYS for which the sum of least square error between the experimental and simulated stress value at each strain point is minimum. And thus finds the best set of values for CYS, C1, D1, C2, D2, C3 and D3=0.

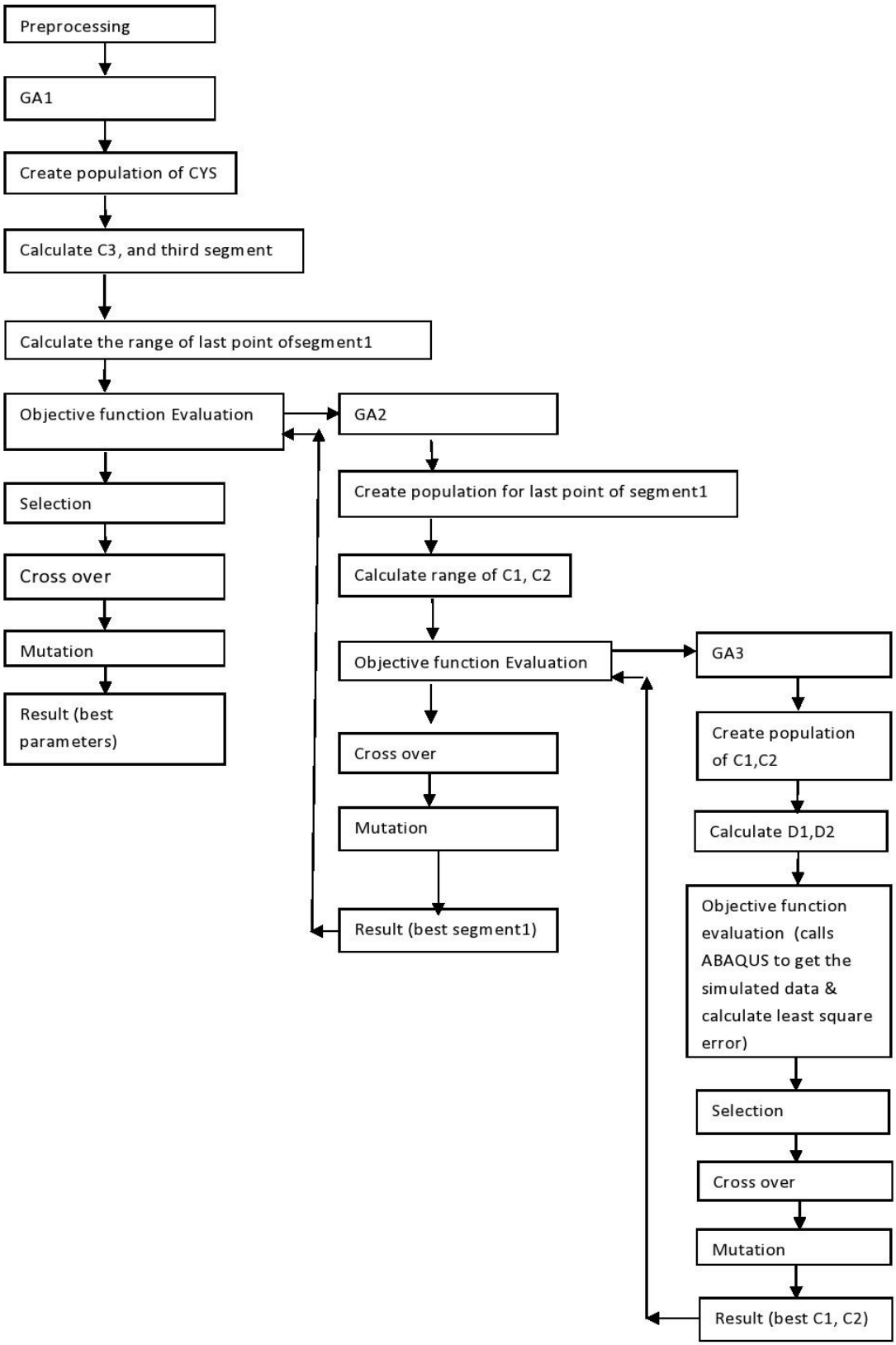

Fig 4.5: *Flowchart for GA based optimization of Chaboche parameters*

Chapter 5. Results and Discussions

5.1 Results

From the tensile tests, the elastic parameters of the material are identified which areused as the inputs for the optimization program. The parameters are rounded to the nearest integer value for the sake of simplicity. The rounded parameters are Young's modulus =210 GPa, and Poisson ratio = 0.3.

The population size for cyclic yield stress ('*GA1*') is10, where maximum 10iterations are to be done. The precision for CYS encoding in set to 1. Similarly, for the optimization ('*GA2*') of the first segment location on the plastic strain axis, the precision is set to $1E-6$, whereas, the population size and maximum number of iterations for GA2 is '5'. The population size and maximum iteration are maintained the same as GA2 for the optimization of $C1$ and $C2$ ('*GA3*') also, though, the precision has been changed to 10 for these parameters. The calculated string length for above selected precisions are 7 for CYS, 10 for *segment1* and 16 for $C1$ and $C2$. The range of the cyclic yield stress is taken as obtained corresponding to 0.01% to 0.05% plastic strain, i. e. $175\ MPa$ to $225\ MPa$.

The best set of parameters value of last five populations is given in table 5.1. And the evolution of hysteresis loop towards the actual experimental loop is shown in fig.5.1.

Table 5.1: *Best set of parameters value of last five populations.*

CYS	C1	D1	C2	D2	C3	D3	RMSE
240	189941	1095	17835	1065	16408	0	40.48
240	294347	3248	17835	1065	16408	0	48.56
211	188137	1093	17959	1069	10069	0	29.94
205	250000	1095	17835	1064	16408	0	51.23
210	204843	1082	17418	986	9957	0	33.05
190	189941	1095	17835	1064	16608	0	26.17

The optimum values of the cyclic yield stress and six kinematic hardening parameters for three-segmented Chaboche kinematic hardening rule is obtained as presented in the Table 5.2. The output variables are also rounded to their nearest integers in the process.

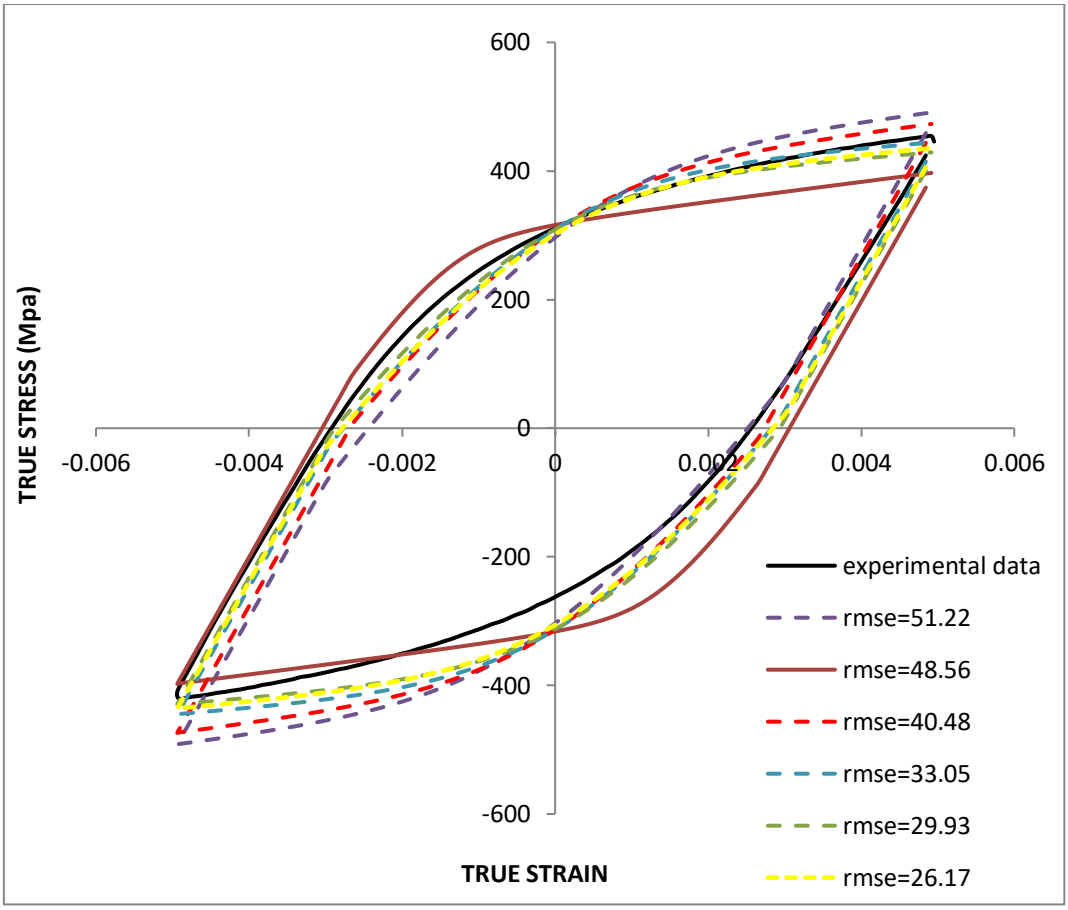

Fig.5.1 Improvement of hysteresis loop with progress in GA iteration.

The optimum material parameters are used to simulate finally and the simulated hysteresis loop is compare with the experimental result. The comparison shows good agreement between them. The comparison is shown in the figure 5.2 below. Here once again it is worth to mention that the developed scheme of sequential GA fully obeys the inter dependence and the constraint equation (eq. 2.1) of Chaboche model as suggested by the Chaboche.

Table 5.2: *Optimized material parameters for Chaboche model*

Material Parameter	**Optimized Value**
CYS (MPa)	190
C1 (MPa)	189941
D1	1095
C2 (MPa)	17835
D2	1064
C3 (MPa)	16608
D3	0

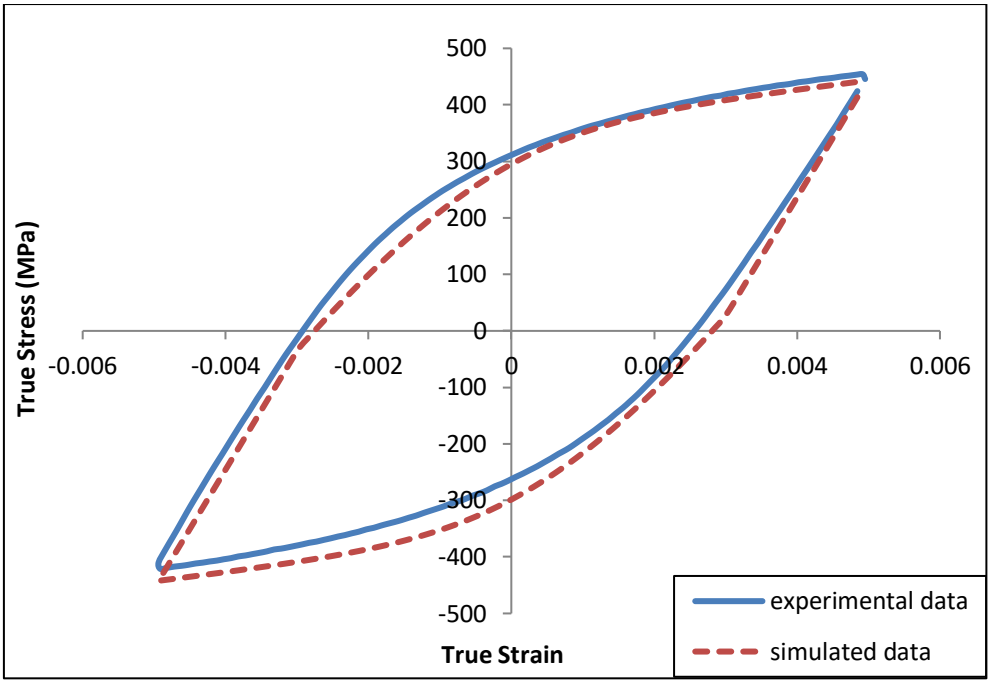

Fig.5.2: *True stress vs. true strain plots for experimental and simulated results, after FE simulation using optimum material parameters.*

5.2 Discussion

As the material parameters are extracted following classical analytical framework and commercially available standard Finite Element package ABAQUS does the simulation, the results are more logically acceptable. The fitness convergence criteria of GA always ensure that the best solution found in any iteration remains until better solution is found.

The above optimization scheme has been planned in such a way (using sequential GA) that it fully obeys the constraints of Chaboche model as proposed by Chaboche. Using a constraint GA scheme with all the parameters as variables, will certainly have some amount of constraint violation.

For the above specified population size and maximum iteration it took $9\ days\ 3\ hours\ 16\ minutes$ to complete the run. The huge computation time is a limitation for such optimization schemes where nested GA routines are involved. If the number of iterations and population size increases, GA may produce better results. Also result depends on the resolution of the available stress-strain data.

The variation of string length of different variables does not affect computational time that much. As for example, the $24\ bit$ string instead of 16 took $3\ s$ extra in a normal computer. It to be mentioned, in this regard that, the invoking of ABAQUS FE environment and maintaining its license checking and other protocols took most of the time. In a normal computer with 4 core CPU with 3.5 GHz processing speed and around $2\ GHz$ data transfer frequency with $32\ GB$ memory and $6\ MB$ Cache, every iteration took $8\ s$.

Chapter 6. Conclusion

6.1 Conclusion

Trial-and-error optimization refers to the process of adjusting variables that affect the output without knowing much about the process that produces the output. A simple example is adjusting the rabbit ears on a TV to get the best picture and audio reception. An antenna engineer can only guess at why certain contortions of the rabbit ears result in a better picture than other contortions. Experimentalists prefer this approach. Many great discoveries, like the discovery and refinement of penicillin as an antibiotic, resulted from the trial-and-error approach to optimization. In contrast, a mathematical formula describes the objective function in function optimization. Various mathematical manipulations of the function lead to the optimal solution. Theoreticians love this theoretical approach.

Generally, when referring to the functional inverse problems for the parameter identification, appropriate objective function must be used in the most calculation procedures. The choice of the function depends on the numerical procedure in material behaviour modelling that will be used. In genetic algorithm for parameter identification random applications were used to solve complex problem. In order to evaluate robustness in such calculation procedure, considering the choice of objective function, the most commonly used functions were examined. The investigation showed extremely good compatibility in results and only very small deviations of simulated from real material's response. Therefore we can conclude that genetic algorithm in parameter identification is robust enough to give reliable data without need to consider the choice of the objective function for inverse problem. The probability to convergence to the accurate results is very high and there is no need for the improvement in the calculation procedure by using specifically oriented objective function.

The choice of various input of the GA like population size, selection criteria, suitable crossover and mutation operator, probability of mutation requires a great insight into the problem. The uniform initialization instead of initial random population generation gives the GA a better performance because there is an individual in each area of the search space. To overcome this randomness, the search space is spitted into subspaces of population size to make each subspace contain an initial individual though it is not easy for multi-dimensional problems.

Use of other advanced material models (Ohno-Wang, 1993; Abdel-Karim/Ohno, 2000; Halama, 2008) may simulate the material behaviour more closely to the actual experimental response.

6.2 Future scope

As the scheme developed in this work does not require any subjective decision in case of material parameter identification so this scheme can be readily used for other materials. **And, the linking of ABAQUS with MATLAB can explore more aspects of the utilization of simulation in other field of design also.**

Various attempts have been devoted to simulate LCF for a single strain range material models, identification of material constants for accurate modelling the material response under cyclic loading within a wide range of strain amplitude is still a challenge. The experiments show that the cyclic stress–strain curves are severely dependent on the strain range for ductile metals. In most of the cyclic material models, only the stabilized cycle is considered to compute the constants of the models. Considering this strategy in the simulation of ductile metals subjected to cyclic loading may lead to erroneous results particularly for the initial cycles of the loading. Each cycle of the hysteresis curve was divided into a tensile and a compressive half cycle. The yield stress and the constants of the three-rule Chaboche kinematic hardening model were computed for each half cycle using an automated program developed based on the genetic algorithm optimization. Therefore, new strain range–dependent relations for isotropic and kinematic hardening conditions may be proposed and the constants of the relations can be computed so that it could accurately simulate the stress–strain curve of the hysteresis loop from monotonic loading to the stabilized cycle.

References

1842, Rankine, W. J. M., On the causes of the unexpected breakage of the journals ofrailway axles, and on the means of preventing such accidents by observing the law ofcontinuity in their construction, Institution of Civil Engineers, Minutes of Proceedings,p105-108.

1854, Braithwaite, F., On the fatigue and consequent fracture of metals, Institution of CivilEngineers, Minutes of Proceedings, p463–474

1864, Fairbairn, W., Experiments to determine the effect of impact, vibratory action and long continued changes of load on wrought iron girders, Philosophical Transactions of theRoyal Society, volume 154, pp311.

1870, Wöhler, A., Über die FestigkeitsversuchemitEisen und Stahl, ZeitschriftfürBauwesen, vol. 20 p73-106

1984, Elline, F., Kujawaski, D., Plastic strain energy in fatigue failure, Journal ofEngineering Materials and Technology Transactions, Volume 106, pp 342-347.

1886, Bauschinger, J., Mechanisch-TechanischenLaboratorium. Materials Forum, 1886.

1988, Wang, Z., Laird, C., Relationship between loading process and Masing behavior incyclic deformation, Materials Science and Engineering: A, Volume 101, Pages L1-L5.

1903, Ewing, J.A., Humfrey, J.C.W., Phil. Trans. Roy. Soc., vol. 200, p241.

1910, Basquin, O.H., Proc. Am. Soc. Testing and Materials 10, p. 625.

1923, Masing, G., ZurHeyn'schenTheorie der VerfestigunVeröffentlichungenausdem Siemens – Konzern, Springer, Berlin, Heidelberg, pp 231-239.

1924, Palmgren, A. A., Durability of ball bearings. 2. Ver. dt.Ing., Volume 68, pp 339.

1928, von Mises, R., Mechanik der plastischenFormänderung von Kristallen, ZeitschriftfürAngewandteMathematik und Mechanik (ZAMM - Journal of Applied Mathematics andMechanics), Volume 8, Issue 3, pp 161-185.

1945, Miner, M. A., Cumulative damage in fatigue, J. appl. Mech., 67, Al59-164.

1947, Taylor, G. I., A Connexion between the criteria of Yield and the Strain RatioRelationship in Plastic Solids, proceedings of the Royal Society A, Volume 191, Issue1027, pp 441-446.

1948, Hill, R., A theory of the yielding and plastic flow of anisotropic metals, Proceedingsof the Royal Society A, Volume 193, Issue 1033, pp 281-297.

1950, Hill, R., Mathematical Theory of Plasticity, Oxford University Press, ISBN: 978-0-198-50367-5.

1950, Drucker, D. C., Stress-strain Relations in the Plastic Range – a Survey of Theory andExperiment, O.N.R. Report, NR-041-032.

1951, Drucker, D. C., A more fundamental approach to plastic stress-strain relations,Proceedings of the First US National Congress of Applied Mechanics, ASME, pp 487-491.

1953, Manson, S.S., Behavior of materials under conditions of thermal stress, NationalAdvisory Committee for Aeronautics, NACA TN-2933

1954, Coffin, L.F., A study of the effects of cyclic thermal stresses on a ductile metal.Transactions of American Society for Testing and Materials 76: 931-950.

1955, Prager, W., The Theory of Plasticity: A Survey of Recent Achievements, Proceedingsof the Institution of Mechanical Engineers, Volume 169, Issue 1, pp 41-57.

1956, Prager, W., A New Method of Analyzing Stresses and Strains in Work HardeningPlastic Solids, Journal of Applied Mechanics, Volume 23, pp. 493-496.

1958, Besseling, J. F., A Theory of Elastic, Plastic and Creep Deformations of an InitiallyIsotropic Material. Journal of Applied Mechanics, Volume 25, pp 529-536.

1959, Drucker, D. C., A definition of stable inelastic material, Journal of AppliedMechanics, Volume 26, pp 101-106.

1961, Mechanical Metallurgy by G.Dieter.

1966,Armstrong, P.J. & Frederick, C.O. A Mathematical Representation of the MultiaxialBauschinger Effect, G.E.G.B. Report RD/B/N, 731.

1979, Essmann, U., Mughrabi, H., Annihilation of dislocations during tensile and cyclicdeformation and limits of dislocation densities, Philosophical Magazine A, Volume 40,Issue 6, pp 731-756.

1979, Chaboche, J. L., Dang Van, K., Cordier, G., Modelization of the strain memory effecton the cyclic hardening of 316 stainless steel, SMiRT-5, Berlin

1979, Chaboche, J.L. & Dang Van, K. &Cordier, G. Modelization of The Strain MemoryEffect on The Cyclic Hardening of 316 Stainless Steel, In: 5th International Conferenceon Structural Mechanics in Reactor Technology, Division L11/3, Berlin, 13.-17. August1979, Ed. Jaeger A and Boley B A. Berlin: Bundesanstaltfür Material prüfung, p.1-10.

1982, Nagtegaal, J. C., On the implementation of inelastic constitutive equations with special reference to large deformation problems, Computer Methods in Applied Mechanics and Engineering, 33, p469-484.

1985, Simo, J. C., Taylor, R.L., Consistent tangent operators for rate-independent elastoplasticity, Computer Methods in Applied Mechanics and Engineering, volume 48, pp101-118.

1986, Simo, J. C., Taylor, R.L., A return mapping algorithm for plane stress elastoplasticity, International Journal for Numerical Methods in Engineering, volume 22, pp649-670.

1989, Chaboche, J. L. & Nouailhas, D. Constitutive Modeling of Ratchetting Effects – Part I:Experimental Facts and Properties of the Classical Models, Journal of EngineeringMaterials and Technology, Vol. 111, p. 384-416.

1989, GOLDBERG, D. E. Genetic Algorithms in Search, Optimization, and MachineLearning. Addison-Wesley, Reading, MA.

1990, J. Lemaitre, J. L. Chaboche, Mechanics of Solid Materials, Cambridge University Press.

1991, Chaboche, J.L. On some modifications of kinematic hardening to improve thedescription of ratcheting effects. International Journal of Plasticity 7, p. 661-678.

1993, Ohno, N. & Wang, J.D. Kinematic Hardening Rules with Critical State of Dynamic Recovery, Part I: Formulation and Basic Features for Ratchetting Behavior, *International Journal of Plasticity* 9, p. 375-390.

1994, Chaboche, J.L. Modelling of ratchetting: evaluation of various approaches.EuropeanJournal of Mechanics, A/Solids 13, p. 501-518.

1995, M. S. E1-Fadaly , T.A. E1-Sarrage, A.M. Eleiche , W. Dahl **,** **"**Fracture toughness of 20MnMoNi55 steel at different temperatures as affected by room-temperature pre-deformation" Journal of Materials Processing Technology 54 , 159-165.

1995, Ypma, T. J., Historical development of Newton-Raphson method, Society for Industrial and Applied Mathematics, Volume 37, Issue 4, pp 531-551.

1996, GEYER-SCHULZ, A. The MIT beer distribution game revisited: Geneticmachine learning and managerial behavior in a dynamic decisionmaking experiment. In Genetic Algorithms and Soft Computing,F. Herrera and J. L. Verdegay, Eds., vol. 8 of Studies in Fuzziness andSoftComputing.Physica-Verlag, Heidelberg, pp. 658–682.

1996, Hideaki Shibata, Hirohisa Shiota. Microstructure dependence of fatigue strength and fatigue crack propagation in titanium aluminide, International Journal of Fatigue, pages 119-125

1997, T. Furukawa, G. Yagawa, Inelastic Constitutive Parameter Identification using an Evolutionary Algorithm with Continuous Individuals, Int. J. Num. Meth. Engng.vol. 40, p.1071-1090.

2000, Bari, S. & Hassan, T. (). Anatomy of Coupled Constitutive Models for RatchetingSimulations. International Journal of Plasticity 16, p. 381-409.

2000, E. Zitzler, K. Deb, and L. Thiele, “Comparisonofmultiobjective evolutionary algorithms: Empirical results,”Evolutionary Computation, vol. 8, no. 2, pp. 173–195.

2000, Chou C.H. and Chen J.N. Genetic Algorithmsinitialization schemes and genes extraction,”Proceeding of the 9th IEEE InternationalConferrence on Fuzzy Systems, Vol. 2, pp.965-968.

2001, X. T. Feng,C. Yang, Genetic evolution of nonlinear material constitutive models, Comp. Meth. Appl. Mech. Eng. Vol. 190, p. 5957-5973.

2002, T. Furukawa, T. Sugata, S. Yoshimura, M. Hoffman, An automated system for simulation and parameter identification of inelastic constitutive models, Comp. Meth. Appl. Mech. Eng., vol 191, p. 2235-2260.

2002, Kobayashi, M., Ohno, N., Implementation of cyclic plasticity models based on a general form of kinematic hardening, International Journal for Numerical Methods in Engineering, 53, p2217-2238.

2004, D. Szeliga, J. Gawad, M. Pietrzyk, Parameter Identification of Material Model Based on the Inverse Analysis, Int. J. Appl. Math. Comp. Sci. vol 14, p. 549-556.

2004, E. K. Burke, S. Gustafson, and G. Kendall, “Diversityin genetic programming: An analysis of measuresand correlation with fitness,” IEEE Transactions onEvolutionary Computation, vol. 8, no. 1, pp. 47–62.

2004,D. Szeliga, J. Gawad, M. Pietrzyk, Parameter Identification of Material Model Based on the Inverse Analysis, Int. J. Appl. Math. Comp. Sci. vol 14, p. 549-556.

2005, R. Fedele, M. Filippini, G. Maier, Constitutive Model for Railway Wheel Steel through Tension-torsion Tests, Comp. Struct. vol 83, p. 1005-1020.

2006, Hyndman, Rob J.; Koehler, Anne B. "Another look at measures of forecast accuracy". International Journal of Forecasting. 22 (4): 679–688. CiteSeerX 10.1.1.154.9771. doi:10.1016/j.ijforecast.2006.03.001.

2006, Rahaman, S. M., Finite Element Analysis and Related Numerical Schemes for Ratcheting Simulation, Ph.D. thesis submitted in North Carolina State University, USA.

2006, Willmott, Cort; Matsuura, Kenji "On the use of dimensioned measures of error to evaluate the performance of spatial interpolators". International Journal of Geographical Information Science. 20: 89–102. doi:10.1080/13658810500286976.

2007, Pook, L. P., Metal Fatigue - What It Is, Why It Matters, Springer, ISBN: 978-1-402-05596-6.

2008, Pontius, Robert; Thontteh, Olufunmilayo; Chen, Hao "Components of information for multiple resolution comparison between maps that share a real variable". Environmental Ecological Statistics. 15 (2): 111–142. doi:10.1007/s10651-007-0043-y.

2008, Halama, R. A Modification of AbdelKarim-Ohno Model for Ratcheting Simulations. *Technical Gazette* 15 (3), p. 3-9. ISSN 1330-3651

2008, J. L. Chaboche, A review of some plasticity and viscoplasticity constitutive theories, Int. J. Plast. vol. 24 no. 10, p. 1642-1693.

2009, M. Franulovic, R. Basan, I. Prebil, Genetic algorithm in material model parameters' identification for low-cycle fatigue, Comp. Mat. Sci., vol. 45 no 2, p. 505-510.

2019, Finite Element Analysis: How to create a great model. *Coventive Composites. 2019-03-18. Retrieved 2019-04-05.*